B.7: RENORMALIZATION in Q.F.T.

Now we come to a central feature of any QFT, and indeed of any physical theory at all, whether it be classical or quantum, and whether it involve fields or particles. As we've already discussed, all theories in physics are "effective theories", in which one focusses on some specific set of degrees of freedom. The idea of renormalization is simply one of transforming between these theories, at the same time changing the size and the meaning of the various parameters in the theories.

We have already seen this on many occasions in our previous discussions. The Landau Fermi Liquid Theory (FLT) is a very nice non-relativistic example, so is the non-linear sigma model (NLS). Non-relativistic physics itself, as we stressed in the last chapter, is simply a low-energy effective version of what becomes QED at higher energies (with the addition of nucleons). And QED is simply the low energy sector of the standard model. In QFT, only gravity stands outside this framework – it is "non-renormalizeable" (we will see what this means), and in some ways fundamentally different from all other QFT's.

In classical physics, as we've already seen, the paradigm for a renormalized theory is hydrodynamics, which "coarse-grains" over short-range fast variables referring to the underlying "granular" structure of a fluid. It only makes sense to devise renormalized theories in classical mechanics when we are dealing with many degrees of freedom; but in QFT, and therefore in ordinary QM, all systems are ultimately many-body in nature. Even in classical mechanics, one can average over the rapid motion of a simple system (eg., over high-ω noise), to get an effective "slow" Hamiltonian.

We have also looked at quite a few techniques for dealing with and implementing this idea. These range from simple perturbation theory to "Born-Oppenheimer" style averaging over fast variables, as well as gradient expansions, and the use of background field techniques. Even the use of $1/N$ expansions, which derives an effective theory, can be thought of as a kind of renormalization.

So what then does renormalization theory give us, in addition to what we already have? We will see that it gives us both new techniques and a new language with which to think about the way we move between different effective theories; and this then allows quite novel ways of thinking about what a physical theory is and what it can do. The techniques also allow us to extrapolate in a meaningful way from simple calculations (such as low-order perturbation theory, or "poor man's scaling", to deduce more general non-perturbative results.

In what follows I begin by discussing 2 naive ways of doing renormalization. One is perturbative, and its use depends on theorems which one has to take on trust in the early stages. The other is naive or "poor mans" scaling, which is easy to implement, and leads already to very important results.

After this, we start a more technical discussion which goes through the details of renormalization. This has a number of different formulations, and here I will focus on both perturbative calculations – used as an input to what is called BPHZ renormalization in relativistic QFT, and to similar schemes in non-relativistic systems – and on the

renormalization group technique (RG). These 2 different techniques involve various technical devices, which I will introduce as we go along - notable amongst these are various regularization devices (the most important of which is dimensional regularization), and ways of doing integrals.

In all of this, one common thread comes through, and is the key to the whole business of renormalization. It is that we start from some theory, which we can think of as the "bare theory", and which consists of a set of degrees of freedom defined in some Hilbert space $\mathcal{H}(E_c)$, which conventionally we will define through its upper UV energy cut-off E_c. We then truncate this Hilbert space, down to a smaller one with UV cutoff Ω_0.

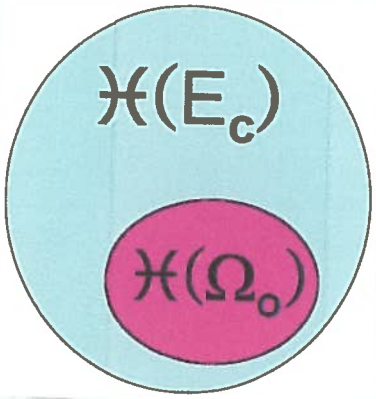

HILBERT SPACES (SCHEMATIC)

The question then is how the theory changes under this change. We are reducing the number of degrees of freedom, and so the original Hamiltonian or Lagrangian or action is now defined for a smaller and different set of modes, with in general different eigenfunctions and different energy levels. The ideas of eigenmodes, and Hilbert spaces for these, may seem a little inappropriate to you if you prefer to think in path integral language - I will come presently to this point.

One of the first questions that one can ask here is - why should the Lagrangian change at all? After all, just because we've thrown away some degrees of freedom in our description doesn't mean that the <u>real system</u>, along with its real eigenfunctions & energy levels, has changed - it is not affected by something we write on paper! However this is to misunderstand what is being done here. To see this, consider the scheme shown in the figure, in which a multi-level system with UV cutoff E_c to a 2-level system with cut-off Ω_0. Thus we go from $\mathcal{H}_{eff}(E_c)$ to $\mathcal{H}_{eff}(\Omega_0)$. The idea then is that these are different; in fact

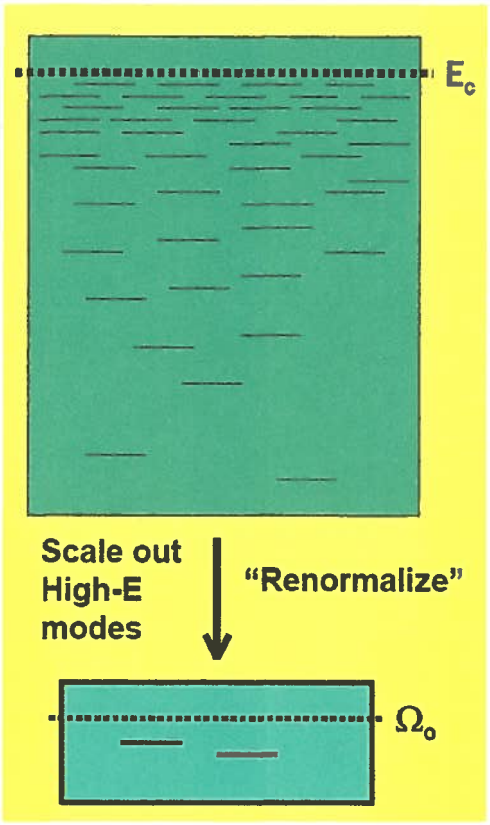

TRUNCATION/RENORMALIZATION

$$\left.\begin{aligned} \mathcal{H}^{(0)}_{eff}(E_c) &= |\psi_i\rangle H^{(0)}_{ij} \langle\psi_j| \\ \longrightarrow \mathcal{H}^{(1)}_{eff}(\Omega_0) &= |\varphi_\alpha\rangle H^{(1)}_{\alpha\beta} \langle\varphi_\beta| \end{aligned}\right\} \quad (1)$$

and the point is that these are different, even for the 2 lowest levels, because in the original Hamiltonian $\mathcal{H}^{(0)}_{eff}(E_c)$, the 2 lowest levels interact with the higher levels, whereas in $\mathcal{H}^{(1)}_{eff}(\Omega_0)$ there are only 2 levels, and they are not allowed to interact with any other levels - the universe is exhausted by these 2 states in the effective 2-level Hamiltonian. By eliminating all interactions with higher levels, we are forced to change the eigenstates and energy levels. In the 1st section of this chapter we will look at toy models to see how this works.

Thinking in this way also allows us to imagine

truncating out the degrees of freedom in incremental steps, rather than in one big jump. It is then clear that each infinitesimal change in the Hilbert space, usually done by making infinitesimal changes in the UV cut-off, will lead to an equally infinitesimal change in the effective Hamiltonian. Now suppose we write our effective Hamiltonians in the form

$$\mathcal{H}_{eff}(\Lambda) = \sum_n g_n(\Lambda)\,\hat{O}_n(\{\varphi_j^\Lambda\}) \qquad (2)$$

where the $\hat{O}_n$ are operators acting on a set of functions $\{\varphi_j^\Lambda\}$, defined in a Hilbert space $\mathcal{H}(\Lambda)$, in which the UV cut-off Λ controls the dimension of the Hilbert space. Then as we change Λ, the relative importance of the different operators will change – the "coupling" $g_n(\Lambda)$ change with Λ as well.

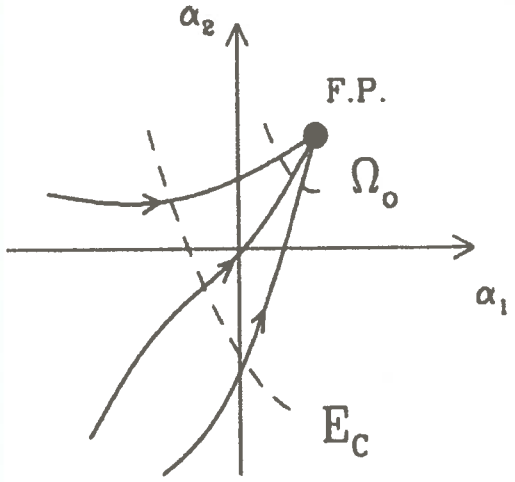

FLOW TOWARD A FIXED POINT IN COUPLING CONSTANT SPACE. FOR UV CUTOFFS E_c OR Ω_0, WE STOP ON LINES

If we then focus on some set of couplings which we consider to be relevant to the problem of interest. The figure shows this in the simple case where we have just 2 couplings, ie., $g_n \to \alpha_1, \alpha_2$. As we change the UV cut-off, these couplings change – we can speak of the continuous "flow" or "RG flow" of the couplings as we change Λ. In the figure this is shown for the case where for a large class of systems, each starting with different values for the initial high-energy couplings, the flow as Λ decreases is always towards a single point, known as the "fixed point" for this class of systems. These flow lines should be seen as representing the evolution of the $\{g_n(\Lambda)\}$ under changes of Λ, ie., as showing the solution of a differential eqtn of form

$$\frac{dg_n(\Lambda)}{d\Lambda} = f(\{g_\alpha(\Lambda)\}, \Lambda) \qquad (3)$$

which describes the flow of the coupling constants – this differential eqtn is the renormalization group eqtn. In principle its behaviour and the solution can be very complicated, but we will see that for many physical systems, the flow takes us, in the low-E limit, to fixed point or fixed lines. The study of the RG structure of a class of effective Hamiltonians turns out to be enormously useful in physics.

One thing you should notice here is that the renormalization is typically being done in one direction, in which it is a UV cut-off that is being lowered, rather than an IR cut-off that is being increased (both have the effect of reducing the size of $\mathcal{H}$, and truncating out degrees of freedom). Why is this? In fact it is a way of expressing the <u>reductionist</u> worldview that has been prevalent in physics for centuries, according to which we build larger objects from smaller building blocks, and not vice-versa (we do not consider the microscopic structure of an object to be derivable or contingent upon its macrostructure). Note, however, that in discussions of quantum measurement, one <u>does</u> make microscopic behaviour contingent upon macroscopic physics!

B.7.1. POOR MAN'S RENORMALIZATION

To do a proper job in renormalization theory, we sometimes have to introduce some fairly complex and sophisticated methods. To get a clear understanding of what is really going on it is then useful to begin by looking at some simple models which are amenable to simpler methods. So in this section we will study a selection of "toy models", and see how far we can get with these simpler methods.

We will be exploring, in these simple models, the 2 main ways in which renormalization is done. The first is perturbative – one tries to guess/infer/deduce the behaviour of the theory by calculating a few graphs, or maybe some class of graphs. This method is more powerful than it looks, for reasons which are not immediately obvious, but which will be explained in this section and in more detail later on. The 2nd method is called "poor man's scaling", and it consists in separating the modes into slow and fast variables, and then integrating out the fast variables to get an effective Hamiltonian/Lagrangian for the slow variables. We've already done this, of course – but now we will do it in a somewhat different way in which we derive an RG eqtn of the form given in (3) above. This will be done with a certain kind of approximation, which is called the "poor man's" scaling method.

These 2 methods are related, as we will see. They are of course not the only ways one can think of to do renormalization, but they give us a good starting point.

B.7.1(a) PERTURBATION THEORY

Going back to our general description of renormalization as given in the intro to this chapter, we see that the simplest way to find the effect, in some low-energy Hilbert space, of the coupling to "virtual states" in a larger Hilbert space, is by doing perturbative expansions. We now see how this works on a variety of models.

(i) MULTI-LEVEL TOY MODELS:

We already mentioned the idea of renormalizing a multi-level model in the introduction. This renormalization of a finite system is about the simplest thing we can imagine doing, and yet its study can be very illuminating. As noted above, the general idea is to truncate out the higher-energy levels, to leave an effective Hamiltonian for some low-E states. ie, we wish to implement in detail the manoeuvre described in eqtn. (1).

2 COUPLED SPIN-½ SYSTEMS (COUPLED QUBITS):

Let's start with a pretty simple system. We have a "high energy" effective Hamiltonian $\mathcal{H}(\vec{\tau}_1, \vec{\tau}_2)$ given by

$$\mathcal{H} = -\tfrac{1}{2}(\Delta_1 \hat{\tau}_1^x + \Delta_2 \hat{\tau}_2^x) - J_0 \hat{\tau}_1^z \hat{\tau}_2^z \qquad (4)$$

where we have a transverse field acting on each "qubit", but a longitudinal interaction acting between them.

Before seeing how we would attack this problem perturbatively, let's note that we can solve it exactly with ease. One finds, for general values of Δ_1, Δ_2, and J_0, that the 4 eigenfunctions are

$$
\left.
\begin{aligned}
|\psi_{++}\rangle &= \left(\frac{\Omega_+ + J_0}{2\Omega_+}\right)^{1/2}\left[\frac{\Delta_1+\Delta_2}{2(\Omega_+ + J_0)}|\uparrow\uparrow\rangle + |\uparrow\downarrow\rangle + |\downarrow\uparrow\rangle + \frac{\Delta_1+\Delta_2}{2(\Omega_+ + J_0)}|\downarrow\downarrow\rangle\right] \\
|\psi_{+-}\rangle &= \left(\frac{\Omega_- + J_0}{2\Omega_-}\right)^{1/2}\left[\frac{\Delta_1-\Delta_2}{2(\Omega_- + J_0)}|\uparrow\uparrow\rangle + |\uparrow\downarrow\rangle + |\downarrow\uparrow\rangle + \frac{\Delta_1-\Delta_2}{2(\Omega_- + J_0)}|\downarrow\downarrow\rangle\right] \\
|\psi_{-+}\rangle &= \left(\frac{\Omega_- - J_0}{2\Omega_-}\right)^{1/2}\left[\frac{\Delta_1-\Delta_2}{2(\Omega_- - J_0)}|\uparrow\uparrow\rangle + |\uparrow\downarrow\rangle + |\downarrow\uparrow\rangle + \frac{\Delta_1-\Delta_2}{2(\Omega_- - J_0)}|\downarrow\downarrow\rangle\right] \\
|\psi_{--}\rangle &= \left(\frac{\Omega_+ - J_0}{2\Omega_+}\right)^{1/2}\left[\frac{\Delta_1+\Delta_2}{2(\Omega_+ - J_0)}|\uparrow\uparrow\rangle + |\uparrow\downarrow\rangle + |\downarrow\uparrow\rangle + \frac{\Delta_1+\Delta_2}{2(\Omega_+ - J_0)}|\downarrow\downarrow\rangle\right]
\end{aligned}
\right\} \quad (5)
$$

where we define

$$\Omega_\pm^2 = J_0^2 + \tfrac{1}{4}(\Delta_1 \pm \Delta_2)^2 \qquad (6)$$

The eigenenergies of the system corresponding to the eigenstates in (5) take the simple form

$$
\left.
\begin{aligned}
E_{++} &= \Omega_+ & E_{--} &= -\Omega_+ \\
E_{+-} &= \Omega_- & E_{-+} &= -\Omega_-
\end{aligned}
\right\} \qquad (7)
$$

and we plot these in the figure as a function of J_0, the inter-qubit coupling.

Now these results are fairly easy to understand, particularly in certain limits - one can then understand things in the whole parameter space by interpolating. We can consider the following limiting cases:

(i) FM limit (J_0 positive; $J_0 \gg \Delta_1, \Delta_2$): In this case we expect the ground state to closely resemble the state $|\psi_{--}\rangle$, which is very closely approximated in this limit by the simple triplet $\frac{1}{\sqrt{2}}(|\uparrow\uparrow\rangle + |\downarrow\downarrow\rangle)$, where the spins are forced to be parallel. The ground state energy is then $E_0 \sim E_{--} \sim -J_0$.

(ii) AFM limit (J_0 negative; $|J_0| \gg \Delta_1, \Delta_2$): Now we expect the ground state to be closely approximated by the singlet $\frac{1}{\sqrt{2}}(|\uparrow\downarrow\rangle + |\downarrow\uparrow\rangle)$, which is most closely mimicked by the state $|\psi_{++}\rangle$. The ground state energy E_0 is again given by $E_0 \sim -J_0$.

(iii) Decoupled limit ($|J_0| \ll \Delta_1, \Delta_2$): When the spins decouple, they are influenced only by the

transverse field acting on each spin; we therefore expect that the ground state will be closely approximated by $|E\rangle \sim |\rightarrow\rightarrow\rangle \equiv \frac{1}{2}[|\uparrow+\downarrow\rangle_1 |\uparrow+\downarrow\rangle_2]$, which is an equal weighting of all the states $|\uparrow\uparrow\rangle$, $|\uparrow\downarrow\rangle$, $|\downarrow\uparrow\rangle$ and $|\downarrow\downarrow\rangle$.

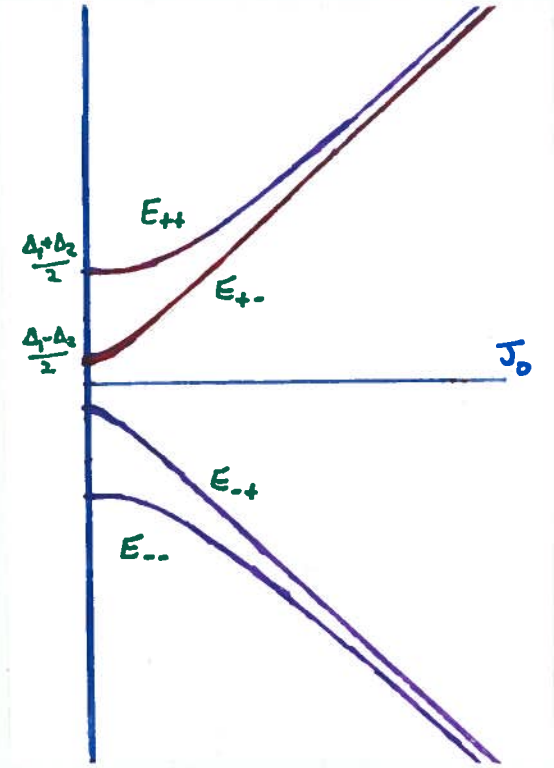

We get a much more detailed picture of what is going on if we look at the time dependence of the problem. This means calculating the time correlation functions — starting the system in some state at time $t=0$, and looking at it again after time t. Thus we can define the propagator

$$G_{\tau_1\tau_2\tau_1'\tau_2'}(t) = \langle\tau_1\tau_2|e^{-i/\hbar\,\hat{H}t}|\tau_1'\tau_2'\rangle \qquad (8)$$

where $\tau_1, \tau_2, \tau_1', \tau_2' = \uparrow, \downarrow$; this defines the amplitude to go from state $|\tau_1'\tau_2'\rangle$ to $|\tau_1\tau_2\rangle$ after a time t. To get a look at this in a graph, without dealing with the complex variables involved, we look instead at

$$P_{\tau_1\tau_2\tau_1'\tau_2'}(t) = |G_{\tau_1\tau_2\tau_1'\tau_2'}(t)|^2 \qquad (9)$$

and in the 1st of 2 figures here we show the function $P_{\tau_1\tau_2}(t) \equiv P_{\tau_1\tau_2\uparrow\uparrow}(t)$, ie, we start the system in state $|\uparrow\uparrow\rangle$, and watch to see what happens; we do this in the strong coupling regime where $|J_0| \gg \Delta_1, \Delta_2$ (the sign of J_0 is not relevant here, but it is convenient to assume that $J_0 > 0$, ie, we are in the strong FM limit).

The results show very clearly a slow oscillation of the system, in this FM limit, between states $|\uparrow\uparrow\rangle$ and $|\downarrow\downarrow\rangle$ at a frequency given by the splitting between the 2 lowest levels.

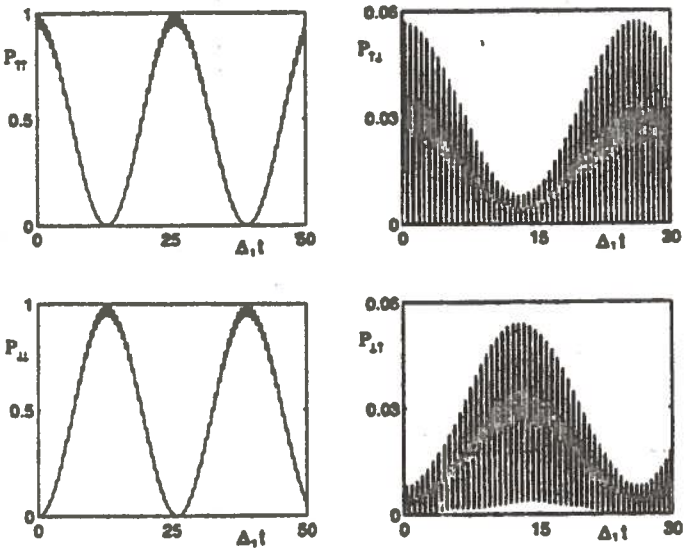

FIG. 1
STRONG COUPLING REGIME
($J_0 \gg \Delta_1, \Delta_2$)

The probabilities $P_{\tau_1\tau_2}(t)$ for a system of spins, coupled by J_0, to start in the state $|\uparrow\uparrow\rangle$ at time $t = 0$, and finish at time t in state $|\tau_1\tau_2\rangle$. We assume $\Delta_2 = 2.5\Delta_1$, and a fairly strong coupling $|J_0| = 5\Delta_1$. $P_{\tau_1\tau_2}(t)$ is plotted as a function of t/Δ_1. Oscillations between the 2 states $|\uparrow\uparrow\rangle$ and $|\downarrow\downarrow\rangle$ occur at the slow "beat" frequency $\Delta_1\Delta_2/2|J_0|$, with very weak high frequency oscillations superposed, coming from the weak mixing with the states $|\uparrow\downarrow\rangle$ and $|\downarrow\uparrow\rangle$. These high-frequency oscillations dominate $P_{\uparrow\downarrow}(t)$ and $P_{\downarrow\uparrow}(t)$, albeit with amplitude reduced by a factor $\sim(\Delta_1+\Delta_2)/2J_0$.

This frequency is equally found to be $\omega = \frac{1}{2}\Delta_1\Delta_2/J_0$, in this limit (it is just $\frac{1}{2}(E_{-+} - E_{--})$).

However we also notice that there is a weak small oscillation superposed on the slow oscillations, of much higher frequency (indeed of frequency $\sim J_0$). These are hardly visible in the probabilities $P_{\uparrow\uparrow}(t)$ and $P_{\downarrow\downarrow}(t)$, but if we look at the "off-diagonal" probabilities $P_{\uparrow\downarrow}(t)$ and $P_{\downarrow\uparrow}(t)$ (which tell us how much of the system is "leaking" out of the low-energy subspace into the 2 high-energy states) we see this more clearly (note however how much smaller is this probability, in comparison with $P_{\uparrow\uparrow}(t)$ and $P_{\downarrow\downarrow}(t)$).

Thus we see very directly in these results how the high frequency states affect the dynamics of the system, if we start it off in the low-energy subspace (and do not start it off in an eigenstate).

In the same way one can look at the case where $|J_0| \ll \Delta_1, \Delta_2$, so that the 2 spins are almost decoupled. As we see in the figure, the effect of J_0 is rather small, and the system spends its time cycling around between all 4 states in roughly equal measure.

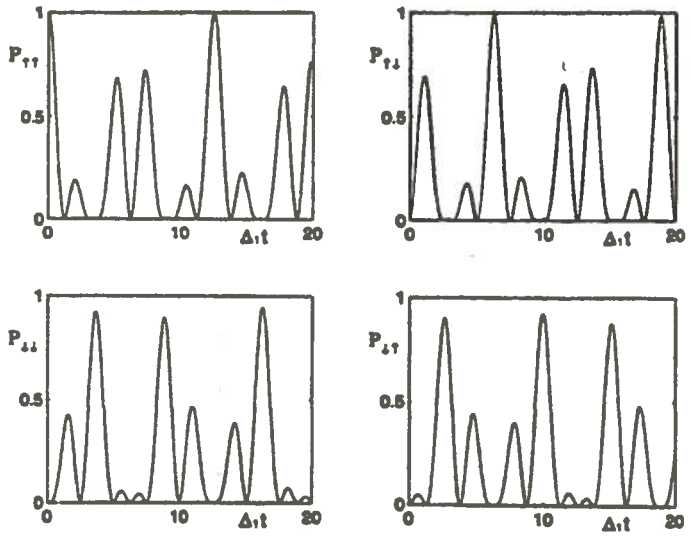

FIG. 2
WEAK COUPLING REGIME
($J_0 \ll \Delta_1, \Delta_2$)

The same probabilities as in ABOVE, but now for weak coupling; we have $\Delta_2 = 2.5\Delta_1$ again, but now $|J_0| = \Delta_1/10$.

The key difference between these 2 cases is of course the fact that there is a clear separation of energy scales in the strong coupling case. It then follows that the 2 subspaces (the high-energy doublet and the low-energy doublet) are largely independent of each other. This is not the case in the weak-coupling regime.

So now let's see how we might have attacked this problem using a perturbative approach. We will do this for the strong-coupling regime, where it makes sense — in fact, we will begin by taking the limit $\Delta_1/J_0, \Delta_2/J_0 \to 0$ and then perturbing about this limit. This is a "strong-coupling expansion", which is an expansion in the "kinetic" terms Δ_1, Δ_2, about the strong-coupling limit. In the limit where $\Delta_1/J_0, \Delta_2/J_0 \to 0$, the ground state of the

system is a degenerate doublet, a linear combination of the states $|\uparrow\uparrow\rangle$ and $|\downarrow\downarrow\rangle$, and the first effect of the perturbation will be to break this degeneracy.

The details of the perturbation calculation are standard. The low-energy subspace can be written in terms of the effective Hamiltonian

$$\left.\begin{aligned} \mathcal{H}_{eff}(\delta J_0) &= |\varphi_\alpha\rangle H_{\alpha\beta} \langle\varphi_\beta| \\ &= (|\uparrow\uparrow\rangle \quad |\downarrow\downarrow\rangle) \begin{pmatrix} 0 & \tilde{\Delta} \\ \tilde{\Delta} & 0 \end{pmatrix} \begin{pmatrix} |\uparrow\uparrow\rangle \\ |\downarrow\downarrow\rangle \end{pmatrix} \end{aligned}\right\} \quad (10)$$

where the renormalized splitting is just

$$\tilde{\Delta} = \frac{\Delta_1 \Delta_2}{2|J_0|} \quad (11)$$

as we already knew - here it is just obtained using 2nd-order perturbation theory; from the lowest degenerate doublet up to the higher doublet (with an energy gap of $2|J_0|$ up to the higher intermediate state. We need the matrix elements Δ_1 and Δ_2 to flip each spin.

This example already shows the basic idea. Lets note again the key step is the truncation from a 4-level matrix to a much simpler 2-level one; in effect we have made the transition detailed in (1), with

$$H_{ij}^{(0)} = \frac{1}{2} \begin{pmatrix} -2J_0 & \Delta_2 & \Delta_1 & 0 \\ \Delta_2 & 2J_0 & 0 & \Delta_1 \\ \Delta_1 & 0 & 2J_0 & \Delta_2 \\ 0 & \Delta_1 & \Delta_2 & -2J_0 \end{pmatrix} \begin{matrix} |\uparrow\uparrow\rangle \\ |\uparrow\downarrow\rangle \\ |\downarrow\uparrow\rangle \\ |\downarrow\downarrow\rangle \end{matrix} \quad (12)$$

$$H_{\alpha\beta}^{(1)} = \frac{1}{2} \begin{pmatrix} 0 & \Delta_1\Delta_2/J_0 \\ \Delta_1\Delta_2/J_0 & 0 \end{pmatrix} \begin{matrix} |\uparrow\uparrow\rangle \\ |\downarrow\downarrow\rangle \end{matrix} \quad (13)$$

where on the right-hand side of the matrix we show the ordering of the states in the matrix

TUNNELING SPIN SYSTEM : We can easily extend the idea discussed above to any multilevel system with a finite number of levels. Common examples include 3-level systems in which either one or two of the levels are at low energy, and the other(s) are truncated out - such models are common in optics.

The case of a tunneling spin S with $2S+1$ levels is of particular interest, because we can use both perturbation theory and WKB/instanton methods on it, and compare the answers - we can even apply RG methods if we wish.

We have already met this system in the last chapter - the Hamiltonian

before truncation is of general form

$$\mathcal{H}(\underline{S}) = \sum_{n=1}^{2S+1} K^{(n)}_{\alpha_1\alpha_2\ldots\alpha_n} \hat{S}^{\alpha_1}\hat{S}^{\alpha_2}\ldots\hat{S}^{\alpha_n} \qquad (14)$$

where $\alpha_j = x, y, z$. We will pick a particularly simple example, where

$$\mathcal{H} = \mathcal{H}_0 + V_0 = -K_0 \hat{S}_z^2 - B_0 \hat{S}_x = -t\left[\frac{k_0}{S}\hat{S}_z^2 + b_0 \hat{S}_x\right] \qquad (15)$$

so that the transverse field B_0 breaks the symmetry w.r.t. rotations about $\hat{z}$.

A complete set of states for this system is provided by the $2S+1$ states $|m\rangle$, where

$$\mathcal{H}_0 |m\rangle = -K_0 S_z^2 |m\rangle = -K_0 m^2 |m\rangle \qquad (16)$$

and it is clear that if the transverse field is weak, we will only slightly mix up these states. If $|V_0| = B_0 S \ll |\mathcal{H}_0| \sim K_0 S^2$, then we expect that the main effect of the perturbation will be to mix the degenerate pairs $|m\rangle$ and $|-m\rangle$ into singlets and triplets, ie, that the eigenstates of $\mathcal{H}(S)$ will be accurately given by states

$$|\pm\rangle_m = \frac{1}{\sqrt{2}}\left(|m\rangle + |-m\rangle\right) \qquad (17)$$

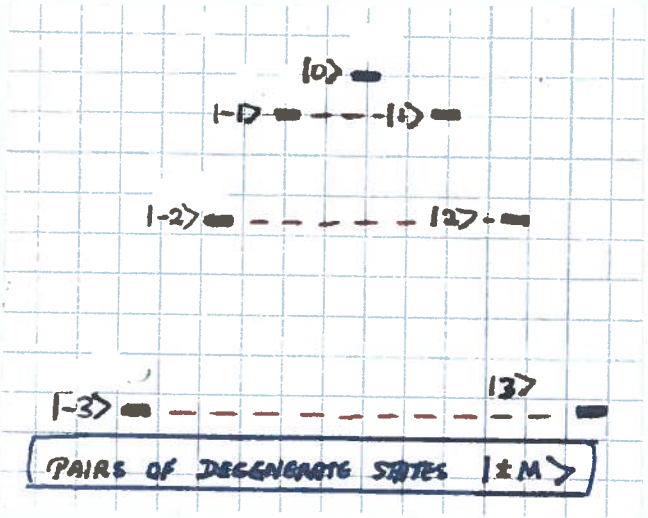

with a splitting which can be calculated - see below. However, if the transverse field is strong, we expect that the levels will be severely scrambled by $\hat{V}_0$, and a given level $|m\rangle$ will couple quite strongly to all the other levels. If we write the Hamiltonian (15) in matrix form, we see how this will work - we have the tridiagonal matrix

$$\begin{pmatrix} -S^2K_0 & -\frac{1}{2}(2S)^{1/2}B_0 & 0 & & & 0 \\ -\frac{1}{2}(2S)^{1/2}B_0 & -(S-2)^2K_0 & -\frac{1}{2}(4S-2)^{1/2}B_0 & & 0 & \vdots \\ 0 & -\frac{1}{2}(4S-2)^{1/2}B_0 & -(S-2)^2K_0 & & & 0 \\ 0 & & & \ddots & & 0 \\ \vdots & 0 & & & -(S-2)^2K_0 & -\frac{1}{2}(2S)^{1/2}B_0 \\ 0 & & & & -\frac{1}{2}(2S)^{1/2}B_0 & -S^2K_0 \end{pmatrix} \qquad (18)$$

where we use the standard result

$$\langle m|\hat{S}_x|m+1\rangle = \tfrac{1}{2}\left[(S-m)(S+m+1)\right]^{1/2} \qquad (19)$$

Now in what follows let's first see what perturbation theory does in general for this problem - and show a few simple examples - and then see how we can think of this in renormalization language.

We begin by defining the matrix element, from (19), as

$$V_0^{m+1,m} = \langle m+1|\hat{V}_0|m\rangle = \tfrac{1}{2} B_0 [(S-m)(S+m+1)]^{1/2} \tag{20}$$

and then calculate the matrix element between the state $|-m\rangle$ and $|m\rangle$ coming from this perturbation on H_0. Applying $V_0 = -B_0 \hat{S}_x$ to the state $|-m\rangle$ repeatedly, we find that this matrix element is

$$\Delta_m = 2\left\{\left[\frac{V_0^{-m,-(m-1)}}{\epsilon^0_{-(m-1)} - \epsilon^0_{-m}} \times \cdots\cdots \times \frac{V_0^{m-2,m-1}}{\epsilon^0_{m-2} - \epsilon^0_m} \; \frac{V_0^{m-1,m}}{\epsilon^0_{m-1} - \epsilon^0_m}\right] + O(V_0^{2m+2})\right\} \tag{21}$$

where the leading term involves a straight sequence of $2m$ transitions between $|-m\rangle$ and $|m\rangle$, and the higher-order terms $\sim O(V_0^{2m+2})$ involve "switchback processes" in which the system retraces its perturbative path one or more times. All of this is shown in the figure, for a transition between states $|-6\rangle$ and $|6\rangle$, in an $S = 7$ system.

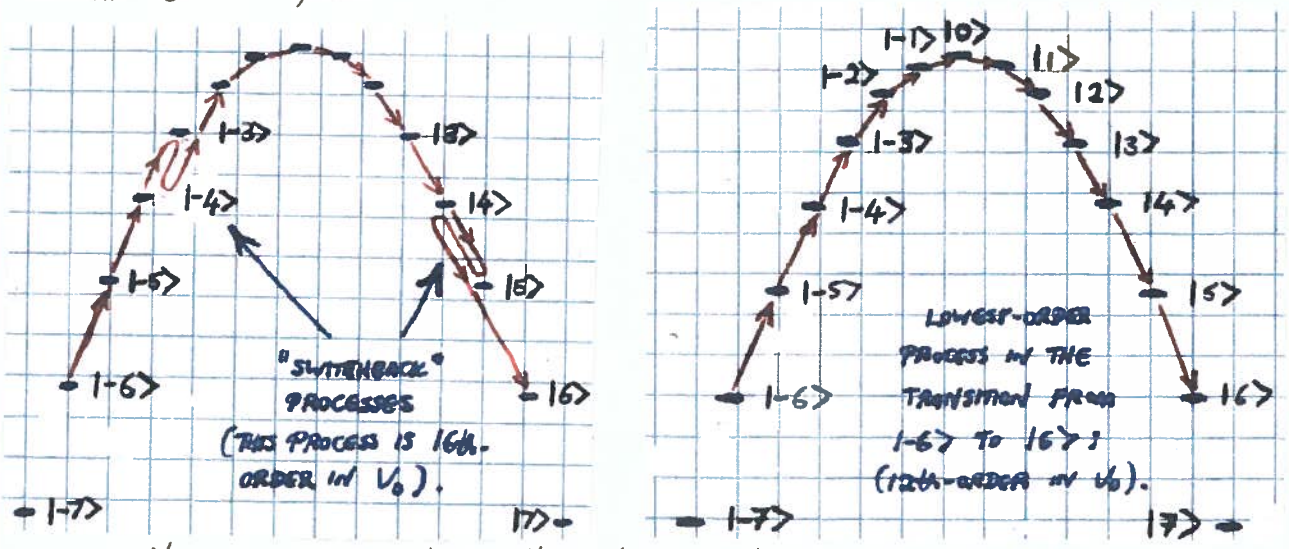

Now we may evaluate the dominant 1st term in (21) by carrying out the product - we have

$$\left.\begin{aligned} \Delta_m &= 2K_0 \left(\frac{B_0}{2K_0}\right)^{2m} \prod_{\ell=-m+1}^{m-1} \frac{1}{m^2-\ell^2} \prod_{\ell'=-m}^{m-1} [(S-\ell')(S+\ell'+1)]^{1/2} \\ &= A_m^S \left(\frac{B_0}{2K_0}\right)^{2m} K_0 + O\left(\frac{B_0}{2K_0}\right)^{2m+2} K_0 \end{aligned}\right\} \tag{22}$$

where the prefactor is

$$A_m^S = \frac{2}{[(2m-1)!]^2} \frac{(S+m)!}{(S-m)!} \tag{23}$$

From the point of view of renormalization theory, the most pertinent case here is that where $n = S$, ie., where we look at the lowest doublet in the system. We then have

$$\left.\begin{aligned} \Delta_S &= \frac{4S(2S+1)}{(2S-1)!}\left(\frac{B_0}{2K_0}\right)^{2S} K_0 \\ &\xrightarrow[S\gg 1]{} \frac{4}{\sqrt{\pi}} K_0 S^{3/2}\left(\frac{eB_0}{4SK_0}\right)^{2S} \end{aligned}\right\} \qquad (24)$$

which, for $S \gg 1$, clearly has a WKB form, ie., we have

$$\Delta_S \xrightarrow[S\gg 1]{} A_S\, e^{-\Gamma_S} \qquad (25)$$

with

$$\left.\begin{aligned} A_S &\sim K_0 S^{3/2} \\ \Gamma_S &\sim 2S \ln\left(\frac{SK_0}{B_0}\right) \end{aligned}\right\} \qquad (26)$$

These results for large S show that the leading perturbative result for $S \gg 1$ just gives the leading WKB result; we glean below at the sub-dominant terms. For small S we can just write down the results:

- $S = 1/2$ (here $H_0 = 0$) Then perturbation theory gives the exact result:

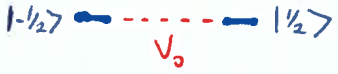

$$\Delta_{1/2} = V_0^{1/2,-1/2} = B_0 \qquad (27)$$

- $S = 1$ Then the transition amplitude Δ_1 between $|-1\rangle$ and $|1\rangle$, from perturbation theory, is

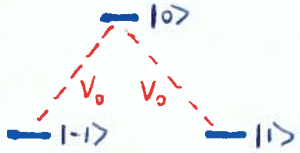

$$\Delta_1 \sim \frac{|V_0^{01}|^2}{\epsilon_0^0 - \epsilon_1^0} = \frac{B_0^2}{K_0} \qquad (28)$$

which is not the exact result – this latter is given by

$$\Delta_1 = \tfrac{1}{2} K_0 \left[\left(1 - 4B_0^2/K_0^2\right)^{1/2} - 1\right] \qquad (29)$$

which tends to the perturbative result (28) in the limit where $B_0/K_0 \ll 1$. This is because (28) neglects all switchback processes. We can continue in this vein:

- $S = 3/2$ We now have

$$\left.\begin{aligned} \Delta_{3/2} &= 3/8\, B_0^3/K_0^2 \\ \Delta_{1/2} &= 2B_0 \end{aligned}\right\} \; S = 3/2 \qquad (30)$$

• $S = 2$ Now we have

$$\left.\begin{aligned} \Delta_2 &= \frac{1}{12} B_0^4 / K_0^3 \\ \Delta_1 &= 3 B_0^2 / K_0 \end{aligned}\right\} \quad S = 2 \qquad (31)$$

and we notice that Δ_1 is larger for $S = 2$ than for $S = 1$; this is because the larger Hilbert space allows more transition pathways.

Note that we don't have to think of this in terms of a spin problem. Suppose instead we just think of some line of sites, with a particle able to hop between them with some matrix element $V^0_{j,j+1}$, which in this case just happens to be given by (20). Then what we are doing here is calculating perturbatively the amplitude $\Delta_{mm'}$ to go between 2 sites m and m'. But there are different ways to make this transition. The first one is shown in the figure as process (a); it is the dominant one in perturbation theory. The process (b) is a switchback process, and contributes to higher order in the perturbation – but note that it never leaves the block of states, labelled M in the figure, which includes $|m\rangle$ and $|m'\rangle$, and all site states in between. There are also processes that go outside this block, and which still contribute to $\Delta_{mm'}$, the total transition amplitude between $|m\rangle$ and $|m'\rangle$. In our spin problem, we have to include such processes when we calculate Δ_M in (22), and they also contribute to the sub-dominant terms in (22).

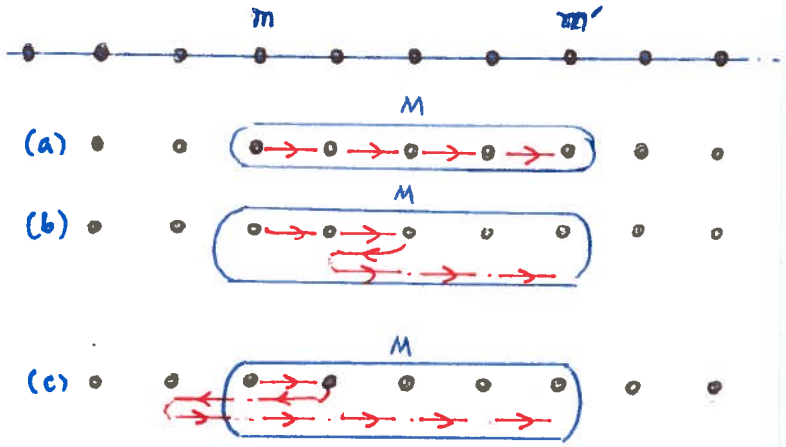

HOPPING PROCESSES BETWEEN SITES m & m' ON A LINE. THE PROCESSES (a) & (b) STAY WITHIN THE BLOCK M OF SITES INCLUDING m & m'. THE PROCESS (c) GOES OUTSIDE M.

Now let's think about all of this in renormalization terms. One way is obvious from what we did before – we can imagine truncating the system to the lowest doublet of states, ie., truncate the Hamiltonian matrix in (18) right down to the qubit effective Hamiltonian

$$\mathcal{H}(\Omega_0) = \begin{pmatrix} 0 & \Delta_S \\ \Delta_S & 0 \end{pmatrix} \qquad (32)$$

with the matrix element Δ_S acting between states $|S\rangle$ and $|-S\rangle$, and the new UV cutoff energy Ω_0 being $\sim K_0 S^2$. This is a standard renormalization to a low-energy effective Hamiltonian; the energy zero is rescaled in (32).

However, we notice that we could do things in quite a different way. Suppose that instead of truncating out all the high-energy levels, we restrict our

truncation to the lowest levels - so that we keep only the high-energy levels, with small $|m|$. Then effectively we are truncating to an effective high-E Hamiltonian, which would make sense under some circumstances — eg., if we were looking primarily at thermal activation processes over the top of the barrier.

We can even go further — suppose we decide to keep only levels $|m\rangle$ and $|-m\rangle$, for some specific value of $|m\rangle$? This amounts to introducing both a UV and an IR cut-off in the problem. This would make sense if, for some reason, only these 2 levels were playing a direct role in the physics (eg., in some resonance process).

The effective Hamiltonians in these 2 cases are obvious from what we did before. We have, eg.,

$$\mathcal{H} = \begin{pmatrix} -\tilde{\epsilon}_1 & \Delta_1 & 0 \\ \Delta_1 & 0 & \Delta_1 \\ 0 & \Delta_1 & -\tilde{\epsilon}_1 \end{pmatrix} \tag{33}$$

in the case where we just keep the 3 highest levels; and we have

$$\mathcal{H}_0 = \begin{pmatrix} \tilde{\epsilon}_m & \Delta_m \\ \Delta_m & \tilde{\epsilon}_m \end{pmatrix} \tag{34}$$

in the case where we just keep the "m-pair" of levels (here the $\{\tilde{\epsilon}_m\}$ are the renormalized levels, shifted from ϵ_m^0; we have not calculated these shifts here).

We can go further in this vein. Suppose we now go over to the site picture discussed above, and imagine isolating "blocks" of states, like the "M-block" described above. Then we can imagine the following approach:

(i) Calculate a renormalized effective Hamiltonian for the M-block states only, in which no transitions to sites outside the M-block are allowed. This means both direct and switchback processes inside the block, but nothing else. We then get an effective $\mathcal{H}$ for the isolated block.

(ii) Then introduce coupling between the block and all other states - we can call these states "the environment" if we wish. This will work fine if we can deal with this coupling perturbatively — it will give a new renormalized Hamiltonian for the M-block.

(iii) Alternatively, we could calculate block Hamiltonians $H_{M_1}, H_{M_2}, \ldots$ for blocks all along the line, and then couple these together perturbatively to get a new renormalized $\mathcal{H}_{\text{eff}}$ for the whole line — but now it has been "coarse-grained", if in doing this we only incorporate the lowest states from each block. This technique is called "Kadanoff scaling" or "block scaling".

Simple ideas like this are at the basis of the whole RG technique, as introduced by Kadanoff & refined enormously by KG Wilson. We shall see how this works as we go along – its power becomes much more obvious when we go over to fields.

(ii) SCALAR FIELD THEORY :

The original formulation of renormalization for QFT, before the idea of RG flow was really understood, was entirely based on perturbation theory, and in fact was technically quite complicated. To see how it works, & how one can try to extrapolate from low-order perturbation theory for a full quantum field, let's look at how perturbation theory is done for a simple scalar field. To be specific we pick the usual ϕ^4 theory, and see what the lowest-order diagrams look like. We will not calculate them (-they are divergent), but this will not yet be necessary – we want instead to understand the relationships between them.

Thus we start again with our old favourite action, viz.,

$$S = \int d^4x \left\{ \tfrac{1}{2}\left[\partial_\mu\phi\partial^\mu\phi - m^2\phi^2\right] - \tfrac{g_0}{4!}\phi^4(x)\right\} \qquad (35)$$

Now, to prepare ourselves for what is coming, let's look at a few lower-order graphs. We first look at graphs for the self-energy – the 2 simplest ones are shown in the figure

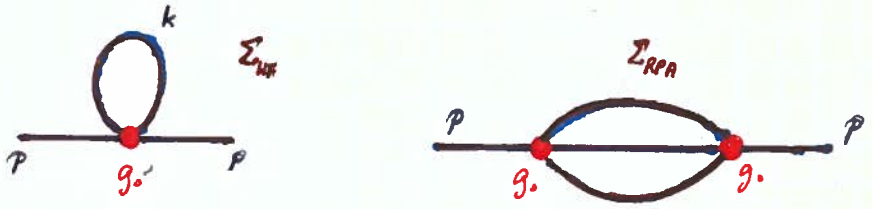

(36)

for which we have the formal expressions

$$\Sigma_{HF}(p) = -\frac{ig_0}{\hbar}\int\frac{d^4k}{(2\pi)^4}\,\frac{i\hbar}{k^2-m^2+i\delta} \qquad (37)$$

$$\Sigma_{RPA}(p) = \left(\frac{-ig_0}{\hbar}\right)^2\int\frac{d^4k}{(2\pi)^4}\int\frac{d^4q}{(2\pi)^4}\,\frac{i\hbar}{k^2-m^2-i\delta}\,\frac{i\hbar}{(k+q)^2-m^2+i\delta}\,\frac{i\hbar}{(p-q)^2-m^2+i\delta} \qquad (38)$$

and we notice that, in the absence of a UV cutoff, the graph for $\Sigma_{HF}(p)$ is divergent – indeed, with a UV cutoff Λ it is $\sim\Lambda^2$, and we say that it is "quadratically divergent". The same is true of the graph for $\Sigma_{RPA}(p)$ in (38). We see this by "power counting"; both graphs have 2 higher powers of 4-momentum in the numerator than in the denominator.

Suppose we now look at some graphs for the 4-point vertex. The lowest

graphs for the 4-point vertex are very familiar to you, and are shown in the figure.

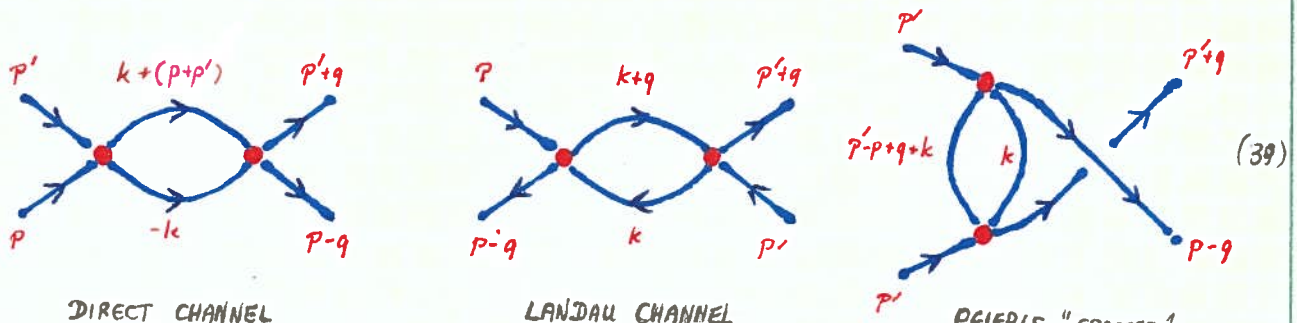

(39)

DIRECT CHANNEL — LANDAU CHANNEL — PEIERLS "CROSSED" CHANNEL

where one should refer back to Chapter 85, eqtns. (170)-(172), for more details. (NB: I have drawn the Peierls diagram a little differently, but one sees from the arguments of the internal lines that it is the same). One sees that the divergences involved are the same for all 3 diagrams. Thus the Landau graph just takes the usual form

$$\Gamma_L(p,p';q) = \left(\frac{-ig_0}{\hbar}\right)^2 \int \frac{d^4k}{(2\pi)^4} \frac{i\hbar}{(k+q)^2 - m^2 + i\delta} \frac{i\hbar}{k^2 - m^2 + i\delta} \tag{40}$$

which we see is logarithmically divergent, ie, with a cutoff Λ we have $\Gamma_L \sim O(\ln \Lambda)$.

We see that for a relativistic QFT with no UV cut-off, we are faced with a rather severe problem of UV divergences (there are no IR divergences here, because the mass $m \to 0$; for massless propagators we have to face these as well). How can we deal with this?

DEGREE OF DIVERGENCE: To understand what to do, we begin by defining the "superficial degree of divergence" of a diagram. What this can be guessed from what we've just done - it refers to the dependence of the diagram on the UV cutoff momentum, and is determined by adding the powers coming into the graph from internal loop integration, any momentum dependence of the interaction itself, and the propagators in the diagram.

For the ϕ^4 theory just discussed above, the superficial degree of divergence is easy to analyze. We've seen that this is 2 for 2-point functions, and 0 for 4-point functions; and if we look at a 6-point graph we quickly find that the degree of divergence is -2, ie., that the integral is quadratically convergent (check for yourself!). So for a ϕ^4 theory, we find the very simple result that the degree of divergence d is given by

$$d = D - n_B \qquad (\phi^4 \text{ theory}) \tag{41}$$

where D is the spacetime dimension (here $D = 4$) and n_B is the number of external legs to the graph.

We can easily generalize this expression to some arbitrary relativistic QFT

involving both fermion lines and boson lines, and with interactions that themselves have some non-trivial momentum dependence, because they involve derivatives ∂_μ of the fields to some power. In what follows, just to simplify things, I will ignore such derivative interactions (it is easy to put them back in) and consider some action of form

$$S[\phi_i, \psi_j] = S_0 + \sum_\alpha S_\alpha [g_\alpha; \phi_i, \psi_j] \tag{42}$$

where the $\{\phi_i\}$ denote different bosonic fields, and the $\{\psi_j\}$ different fermionic fields; the term S_0 is the free field term, with no couplings in it. Now each of the S_α will in principle involve different couplings, having different powers of the fields in it.

Let's now define the following quantities, for a given diagram

No. of external fermion legs :	n_F
No. of external boson legs :	n_B
No. of internal fermion lines :	l_F
No of internal boson lines :	l_B
No. of intenal vertices of type α :	N_V^α
fermionic power in vertex type α :	P_F^α
bosonic power in vertex type α :	P_B^α

(43)

To see what is meant by this, consider the graph shown in the figure, which describes a 6-point vertex $\Gamma^{\psi\psi\phi}_{42}$ for interacting fermion-boson theory.

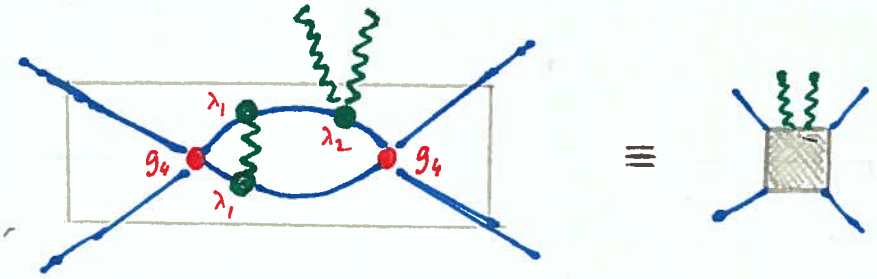

(44)

Note that we have 3 different interaction terms in this theory. There is a 4-fermion interaction g_4, plus an interaction between 2 fermions and either a single boson, or a pair of boson; we thus have

$$S_0 = S_0 + \int d^D x \left\{ g_4 (\bar\psi\psi)^2 + \lambda_1 (\bar\psi\psi\phi) + \lambda_2 (\bar\psi\psi\phi^2) \right\} \tag{45}$$

and these 3 interaction terms (with $\alpha = 1,2,3$) have $P_F^\alpha = 4,2,2$, and $P_B^\alpha = 0,1,2$, respectively. In the diagram in the figure, we also have $n_F = 4$, $n_B = 2$, $l_F = 2$, $l_B = 1$, and we have $N_V^\alpha = 2,2,1$ for $\alpha = 1,2,3$.

We can now establish some simple general results for the degree of divergence of an arbitrary graph for some theory. It is easy to see that

$$d = D\left(1 - \sum_\alpha N_V^\alpha\right) + (D-2) l_B + (D-1) l_F \tag{46}$$

We get (46) by noting the following: first, every internal vertex comes with a delta-function of momentum variables, in D spacetime dimensions; this would give a factor $-\sum_\alpha D N_V^\alpha$, but the δ-function integration which gives overall momentum conservation should not be included in the sum. Then for every internal boson line we have a D-dimensional integration, but with an integrand $\sim O(1/k^2)$, giving a factor $D-2$; and every fermion line has an integrand $\sim O(1/k)$, giving $D-1$. Hence we get (46).

Another way to write this formula is obtained by noting that

$$\left.\begin{aligned} n_B + 2l_B &= \sum_\alpha N_V^\alpha P_B^\alpha \\ n_F + 2l_F &= \sum N_V^\alpha P_F^\alpha \end{aligned}\right\} \qquad (47)$$

which arise because every external boson/fermion line is attached to one vertex, and every internal line to 2 vertices; summing over all lines we get (47). Substituting this into (46), we get

$$d = D - \frac{D-2}{2} n_B - \frac{D-1}{2} n_F + \sum_\alpha N_V^\alpha \Delta_\alpha \qquad (48)$$

where Δ_α is the "index of divergence", given by

$$\Delta_\alpha = \tfrac{1}{2}\left[(D-2) P_\alpha^B + (D-1) P_\alpha^F\right] - D \qquad (49)$$

To take two simple examples, we have

- For ϕ^4 theory, the index of divergence $\Delta_\alpha = 0$; the 4-boson interaction has $P_\alpha^B = 4$, and $P_\alpha^F = 0$ because there are no fermions; thus we get $\Delta_\alpha = \Delta_{\phi_4} = 0$ when $D = 4$. We then immediately recover the result given in (41) above for ϕ^4 theory in 4 dimensions – the degree of divergence depends only on the number of external legs. Note however that this is only true when $D = 4$; thus, eg., when $D = 3$, then $\Delta_{\phi_4} = -1$, and the degree of divergence of any graph depends not only on n_B, but also on the number of internal vertices N_V.

- For the graph given in the figure (44), we have a degree of divergence $D-4$; this is easy to see using power counting, and one can also recover it using (48) and (49).

Thus we see that any diagrammatic expansion will be full of divergences, of different degrees.

SUBTRACTIONS & GRADIENT EXPANSIONS: Although the various vertices in a relativistic QFT are, as we've seen, very often divergent, their behaviour is otherwise not so complicated to understand. We can see this if we again consider the 2-loop graph $\Sigma_{RPA}(p)$ in (36). Although this is quadratically divergent, there is nothing to stop us performing a gradient expansion (which here becomes an expansion in powers of p) around some specific value of p; the simple

pole structure of the integrand makes such a expansion straightforward (using, eg., a partial fraction expansion).

The general form that such an expansion will take is then

$$\Sigma(p^2) = \Sigma(p_0^2) + (p^2-p_0^2)\left.\frac{\partial\Sigma}{\partial p^2}\right|_{p^2=p_0^2} + \Delta\Sigma_{p_0}(p^2) \tag{50}$$

where p_0 is some arbitrary momentum around which we expand, and we write everything in terms of p^2 because everything is an even function of p (and of m).

The basic idea now is to choose $p_0 = \tilde{m}$, the "physical mass", ie., the low-energy limiting mass of the theory - assuming there is such a limit. We then see that the physical mass must be given by

$$\tilde{m}^2 = m^2 + \Sigma(\tilde{m}^2) \qquad \text{[MASS RENORMALIZATION]} \tag{51}$$

ie., that m is renormalized to $\tilde{m}$ by Σ; this is a self-consistent eqtn. for $\tilde{m}$. We can then write

$$\left.\begin{aligned} G_2(p) &= \frac{i}{\left[1-\partial\Sigma/\partial p^2\big|_{\tilde{m}^2}\right](p^2-\tilde{m}^2) - \Delta\Sigma_{\tilde{m}}(p^2) + i\delta} \\ &\equiv \frac{i Z_\phi}{(p^2-\tilde{m}^2) - \tilde{\Sigma}(p^2) + i\delta} \end{aligned}\right\} \tag{52}$$

where the factor Z_ϕ is called the wave-function or field renormalization factor, and is

$$Z_\phi = \frac{1}{1-\partial\Sigma/\partial p^2\big|_{p^2=\tilde{m}^2}} \qquad \text{[FIELD RENORMALIZATION]} \tag{53}$$

and where it is also incorporated into the renormalized self-energy, ie., we have

$$\tilde{\Sigma}(p^2) = Z_\phi\,\Delta\Sigma(p^2) \tag{54}$$

The name for mass renormalization is fairly obvious from its definition in (51). That Z_ϕ is a field renormalization is clear from the definition of $G_2(p)$, which is quadratic in the field operators ϕ_p. Thus if we define a renormalized field

$$\tilde{\phi}(x) = \frac{1}{\sqrt{Z_\phi}}\,\phi(x) \tag{55}$$

then we have

$$G_2(p) = \frac{1}{Z_\phi}\,G_0(p) \tag{56}$$

where the bare propagator $G_0(p)$ is, as usual, given by

$$\left.\begin{aligned} G_0(p) &= i\hbar\,\Delta_F(p) = \frac{i\hbar}{(p^2-m^2)+i\delta} \\ &\equiv \int d^4x\, e^{-ip\cdot x} \langle 0|T\{\phi(x)\,\phi(0)\}|0\rangle_{bare} \end{aligned}\right\} \quad (57)$$

Thus we establish that, given a well-behaved expansion for the 2-point vertex around some fixed momentum, we can define a renormalized vertex having the same form as the bare propagator, but with renormalized parameters. Two points are important here:

- In a relativistic QFT like ϕ^4 theory, these renormalizations are infinite, because of the divergences. Thus in (51), we have a finite physical mass m_0; but since $\Sigma(m_0^2)$ is in general infinite, this implies that m^2 is also (with the opposite sign). The same is true of Z_ϕ^{-1}. That these infinities exist is not surprising — they come because the original fields and masses refer to fields defined up to infinite energy.

- The basic form of the renormalization has nothing to do with the issue of divergence — at no point did the divergences enter the discussion from eqns (50)-(56). In fact we have seen all of this before, in the discussion of Fermi liquid theory in Chapter 5, where both the wave-function renormalization and the changes in $\Sigma(p)$ were finite. This finiteness arose simply because in any condensed matter effective Hamiltonian, a finite UV cut-off emerges naturally.

From this latter perspective it is clear that it is physically meaningless to be integrating up to infinite momenta in the internal states in a diagram. As we've already emphasized several times, any action like a ϕ^4 action has to be viewed as an effective action, only valid over a certain energy range — it then makes no sense to integrate outside this energy range.

COUNTERTERMS & BPHZ RENORMALIZATION: So far we have seen how one might set up a renormalization scheme, even in the presence of divergences; but there is still no reason to assume that this is capable of dealing with all diagrams. Thus, in dealing with the ϕ^4 theory, we have seen how one might consistently renormalize the 2-point vertex, by introducing 2 (infinite) renormalization constants. But what about all the other vertices — do we have to now introduce a new set of renormalization constants for each new vertex (ie, 4-point, 6-point, etc). A theory with an infinite set of renormalization constants is no theory at all.

This turns out not to be the case if we have a <u>renormalizable theory</u>. A good way to set up the whole structure was pioneered by

Bogolimbov, with later refinements and generalization by Parusiak, Hepp, & Zimmermann. The idea of counterterms was first introduced in order to make the smooth link between the bare Lagrangian and the renormalized one.

The basic idea is fairly simple. Suppose that in doing a few lower order calculations of diagrams we find that the results for the lowest vertex parts can be rewritten in renormalized form as shown above, with a shifted mass, wave-function renormalization, and a renormalized coupling (these being the 3 relevant objects in the ϕ^4 theory). Now, the argument goes, let's make these shifts before we even start the calculation. In other words, lets add terms to the original action which already make these shifts.

For the ϕ^4 Lagrangian it is completely obvious how to do this. We simply write a new action

$$\tilde{S} = S - \int d^4x \left\{ \tfrac{1}{2}[A\partial_\mu\phi\partial^\mu\phi - B\phi^2] - C/4!\,\phi^4 \right\} \qquad (58)$$

where A, B, and C are determined by low-order calculations of graphs. In the case of ϕ^4 theory, these constants are given by defining the new renormalized quantities $\tilde{m}$, $\tilde{\phi}$, and $\tilde{g}$, so that

$$\tilde{S}[\tilde{\phi}] = \int d^4x \left\{ \tfrac{1}{2}[\partial_\mu\tilde{\phi}\partial^\mu\tilde{\phi} - \tilde{m}^2\tilde{\phi}^2] - \tilde{g}/4!\,\tilde{\phi}^4 \right\} \qquad (59)$$

with the renormalized quantities adjusted to agree with the physical quantities. This then fixes A, B, and C; we have

$$\left.\begin{aligned} \tilde{\phi}(x) &= \phi(x)\sqrt{1+A} \\ \tilde{m}^2 &= \frac{m^2+B}{1+A} \\ \tilde{g} &= \frac{g+C}{(1+A)^2} \end{aligned}\right\} \qquad (60)$$

So far so good. But now the obvious question is - how do we know that this will work when we calculate any other graph, or when we do a graphical sum? There are a number of things that could easily go wrong; here are some of them:

(1) The results for the renormalization in (60) seem natural enough; we have a field renormalization $\sqrt{1+A} \equiv Z_\phi^{-1/2}$, and the mass and coupling constant also contain this factor (squared for $\tilde{m}^2$, and to the 4th power for $\tilde{g}$, because these vertices have 2 and 4 external legs respectively). Otherwise we simply shift $\tilde{m}^2$ and g by constants (which happen to be infinite). So what now happens when we calculate, say, the contributions to the 6-point or 8-point vertices? There are clearly 2 possible things that might ensue; either we generate new kinds of renormalization, and then we will need to include further terms in $\tilde{S}$ of order ϕ^6, ϕ^8, etc; or we will find that the renormalized vertices for these

higher contributions can all be understood in terms of the three renormalizations that we already have in (60). Thus the question boils down to the consideration of the graphs shown in the figure, and others like them, for contributions to Γ_6, and so on:

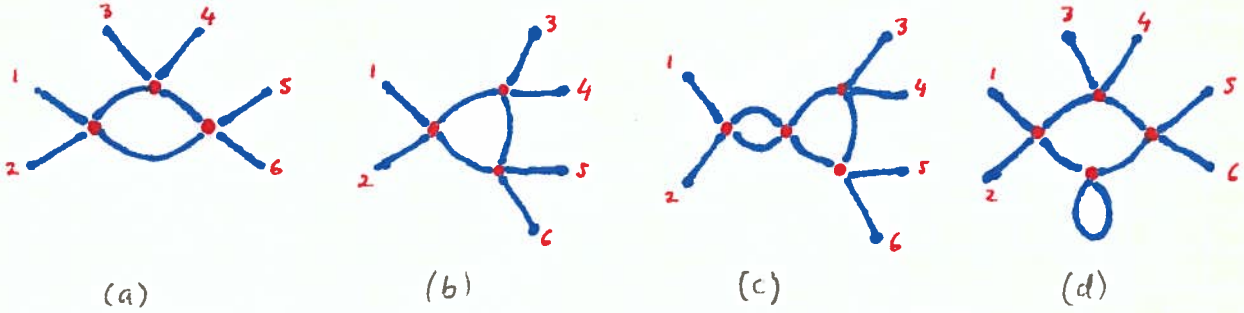

(a) (b) (c) (d) (61)

All of these graphs contribute to $\Gamma_6(1,2,\ldots 6)$; but the real question we are trying to answer is - do they require us to add a term like

$$\delta\tilde{S}_6[\phi] \sim \int d^4x\ \mathcal{D}\phi^6(x) \qquad (62)$$

to our effective action, or is the form (59) good enough? Note that all of the graphs in (61) are superficially convergent, from our original result (47); divergence is not the issue here. Note also that graph (d) in (61) just involves a simple self-energy insertion in (a), so we don't expect it to be independent of (a). However (b) and (c) obviously have a different structure from (a) and (d).

(ii) A separate question — what about divergences in higher order graphs? In ϕ^4 theory we have seen that higher vertices (6-point, 8-point, etc) are not divergent. But what about higher contributions to the 2-point and 4-point functions — how do we know that they will not contain different kinds of divergence from the ones we have already looked at in lowest-order perturbation theory? Thus, consider the graphs shown here for the 2-point vertex $\Sigma(p)$; what reason do we have to suppose that, even if these do not change the <u>form</u> of $\tilde{S}$, with 3 counterterms, that they will not considerably change the form of the counterterms? Notice that (a) involves an overlap of 2 graphs we've already seen (cf. (36)b); and (b) below involves insertions of 6-point vertex diagrams from (61) above.

(a) ; (b) ; etc. (63)

These questions (and others) are not so easy to answer, and they require the full apparatus of renormalization theory. To give proper answers, therefore, lies beyond the scope of the "poor man's" theory we are doing here. However, we can summarize

the conclusions of all of this work by distinguishing between 3 possible classes of theory.

(a) SUPER-RENORMALIZABLE THEORY : In this case, by definition, the index of divergence Δ_α defined in eqtn (49) is negative, ie., we have

$$\Delta_\alpha < 0 \qquad \text{(SUPER-RENORMALIZABLE)} \tag{63}$$

for all of the different terms in the action. In this case the total number of divergent graphs is actually finite - so we can catalogue these different divergences and after that everything is finite. An example of a super-renormalizable theory is the ϕ^3 scalar field theory in $D = 4$ spacetime dimensions, where $\Delta = -1$. It is easy to see that there is a small number of graphs that diverge for this theory. Notice that for ϕ^3 theory, in 4 dimensions, we have a degree of divergence for any graph given by

$$\left.\begin{aligned} d &= D - n_B + \Delta \\ &= 3 - n_B \end{aligned}\right\} \quad (\phi^3 \text{ theory, } D = 4) \tag{64}$$

and so the only graphs having any divergences will be 2-point and 3-point graphs.

(b) RENORMALIZABLE THEORY : In this case we have a dividing line between 2 cases; by definition, a renormalizable interaction with coupling g_α has

$$\Delta_\alpha = 0 \qquad \text{(RENORMALIZABLE)} \tag{65}$$

In this case, which we have already seen with ϕ^4 theory in 4-d, the degree of divergence d for graphs for some vertex part is independent of the number of internal vertices. If the lower-order graphs are divergent, then so will the higher-order graphs be so. However, crucially, we only have a finite number of different kinds of divergence. This means that the "counterterm" procedure of Bogoliubov's will work - if we now calculate with the renormalized Lagrangian, then everything will come out finite.

(c) NON-RENORMALIZABLE THEORY : In this case, the most problematic, we have a positive index of divergence, ie., we have

$$\Delta_\alpha > 0 \qquad \text{(NON-RENORMALIZABLE)} \tag{66}$$

for some interaction with coupling g_α. In this case, the degree of divergence d increases as we increase the number of g_α-vertices in our diagrams, and therefore any diagram, no matter how many external legs it has, will become divergent at sufficiently high order in g_α. An example is ϕ^5 or ϕ^6 theory. One then finds that we need an infinite number of counterterms to deal with these divergences - the theory becomes apparently useless.

The definitions & results we have established so far constitute the bare bones of renormalization that was current in the early to mid-1960's. Even though we deal with the general properties of diagrams, the theory is nonetheless firmly rooted in perturbation theory. With this limitation, it was nevertheless a powerful tool, particularly when applied to a large variety of different models in particle physics.

However what was not at all clear from all of this was the more general framework in which one should understand renormalization, beyond perturbation theory. A great advance was made with the development of renormalization theory, to which we now turn.

B.7.1.(b) RENORMALIZATION GROUP : INTRO

Many books have been written on different aspects of the theory and applications of the renormalization group (RG), in both particle physics and condensed matter theory (and, more recently, in areas ranging from finance and economics to pure mathematics. In what follows I will not even remotely attempt to cover all of this, but instead give an understanding of the key ideas, and of how to do certain kinds of calculation.

What I will do is begin with 3 examples which give some idea of how it all works. We will then go on to give a more general treatment. The examples are (i) a simple impurity scattering model in non-relativistic physics; (ii) the Berezinskii / Kosterlitz-Thouless, which applies to many different physical systems; and finally (iii) the ϕ^4 system, which is the example used by KG Wilson to develop much of the theory.

(i) IMPURITY SCATTERING :

The following example is very simple, and it allows us to see how the RG can work without all the complexity involved in a QFT example.

Consider a Hamiltonian

$$\mathcal{H}_0 = \sum_k \epsilon_k^0 c_k^\dagger c_k + V_0 \delta(\underline{r}) \tag{67}$$

where the free-particle energy is confined to a band:

$$\epsilon_k^0 = \epsilon_k \, \theta(D_0 - |\underline{\epsilon}_k|) \tag{68}$$

so that in k-space, the δ-fn. potential has the form

$$\left.\begin{aligned} V_{kk'} &= V_0 \, \theta(D_0^2 - \epsilon_k^2)\, \theta(D_0^2 - \epsilon_{k'}^2) \\ V(\epsilon, \epsilon') &= V_0 \, \theta(D_0^2 - \epsilon^2)\, \delta(\epsilon - \epsilon') \end{aligned}\right\} \tag{69}$$

where the factor $\delta(\epsilon-\epsilon')$ arises because the scattering is elastic. Now we can easily write down an expression for the 1-particle propator for this problem; one has

$$\mathcal{G}_{kk'}(\epsilon) = G^0_k(\epsilon) + G^0_k(\epsilon)\, T_{kk'}(\epsilon)\, G^0_{k'}(\epsilon) \tag{70}$$

where the T-matrix is

$$T_{kk'}(\epsilon) = \sum_{k''} V_{kk''}\left(1 - G^0_{k''}(\epsilon)\, V_{k''k}\right)^{-1} \tag{71}$$

Since the scattering here is S-wave, we can go to a scattering channel representation, and drop the momentum indices entirely. We can then write the T-matrix as

$$T_{kk'}(z) \to T_0(z) = \frac{V_0}{1 - V_0 \sum_{k\in D_0} \frac{1}{z-\epsilon^0_k}} \tag{72}$$

$$\equiv \frac{V_0}{1 - V_0 \int_{-D_0}^{D_0} d\epsilon\, \frac{N(\epsilon)}{z-\epsilon}} \tag{73}$$

where z is a complex frequency, and where $N(\epsilon)$ is just the density of states. In the simple case where $\epsilon_k = v_F k$ (flat density of states, ie $N(\epsilon) \to N_0$) we have

$$T_0(E+i\delta) \underset{N(\epsilon)\to N_0}{\longrightarrow} V_0\left[1 - V_0 N_0\left(\ln\left|\frac{D_0 - E}{D_0 + E}\right| - i\pi\,\theta(D_0^2 - E^2)\right)\right]^{-1} \tag{74}$$

which essentially constitutes an exact solution to the problem. In such scattering problems it is common to write things in terms of a phase shift; one has

$$\delta_0(E) = \tan^{-1}\left(\frac{\pi V_0 N(\epsilon)}{1 - V_0 \int_{-D_0}^{D_0} d\epsilon\, \mathcal{P}\frac{N(\epsilon)}{E-\epsilon}}\right) \underset{N_\epsilon = N_0}{\to} \tan^{-1}\left(\frac{\pi V_0 N_0}{1 - V_0 N_0 \ln\left|\frac{D_0 - E}{D_0 + E}\right|}\right) \tag{75}$$

It is useful to draw some pictures here. Notice first that the simple T-matrix eqns in (70) and (71) have the graphical representation:

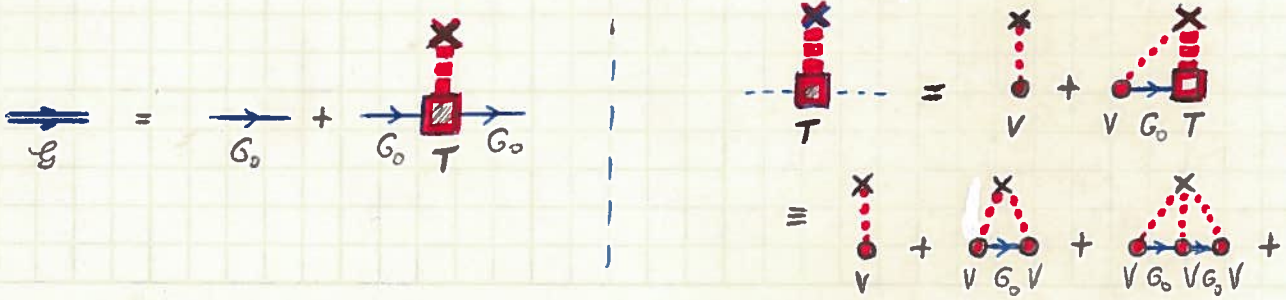

which we will come back to later once we start renormalizing. Note that we can also now write the propagator as

$$\mathcal{G}(z) = \frac{1}{G_0^{-1}(z) - \Sigma(z)} = \frac{1}{G_0^{-1}(z) - T_0(z)} \equiv \frac{1}{z - \epsilon_k^0 - T_0(z)} \qquad (7)$$

in this isotropic scattering case.

So far so good - this is just standard quantum mechanics. It is useful to draw pictures of the key quantities $\delta_0(E)$ and $\tan\delta_0(E)$, which characterize both the scattering rate and energy shift caused by the scattering. In these figures I show this both for the case of a flat band, and for a more general band:

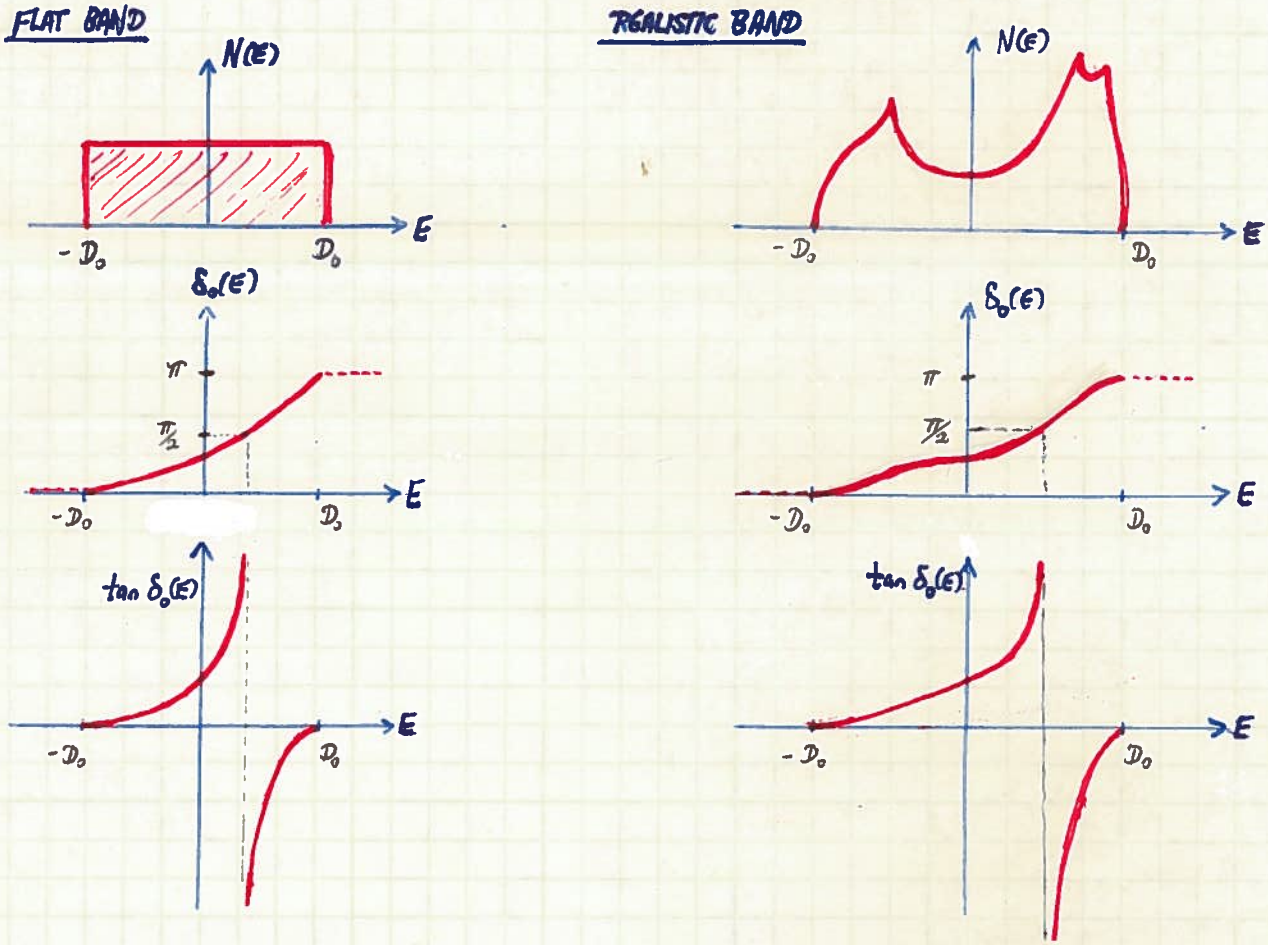

As we will see, the key quantity involved in renormalization will be $\tan\delta_0(E)$, which gives an energy shift; we have

$$\tan\delta_0(E) = \frac{\mathrm{Im}\, T_0(E)}{\mathrm{Re}\, T_0(E)} \qquad (77)$$

Now to carry out the renormalization, we will do what was illustrated schematically in the intro to our discussion of renormalization, ie., we will carry out a sequence of truncations of the Hilbert space for the system, as follows

$$\left.\begin{aligned}
&\mathcal{H}_0 \Rightarrow \mathcal{H}_1 \;; \quad (-D_0 < \epsilon < D_0) \Rightarrow (-D_1 < \epsilon < D_1) \\
&\mathcal{H}_1 \Rightarrow \mathcal{H}_2 \;; \quad (-D_1 < \epsilon < D_1) \Rightarrow (-D_2 < \epsilon < D_2) \\
&\quad\vdots \\
&\mathcal{H}_{n-1} \Rightarrow \mathcal{H}_n \;; \quad (-D_{n-1} < \epsilon < D_{n-1}) \Rightarrow (-D_n < \epsilon < D_n) \\
&\text{etc} \qquad\qquad\qquad\qquad\qquad\qquad \text{etc}
\end{aligned}\right\} \quad (78)$$

where $D_0 > D_1 > \cdots D_n > \cdots$, etc.; we continue to slice bits off the outer edges of the band, to reduce progressively the size of the Hilbert space, and go to the low-energy limit.

To do this in practice, let's write the truncation as follows. Let's write

$$\delta G_0(z) = \left[\int_{-D_0}^{-D_1} d\epsilon + \int_{D_1}^{D_0} \epsilon \right] \frac{1}{z-\epsilon} \quad (79)$$

as the contribution to $G_0(z)$ from the parts cut out in going from $\mathcal{H}_0$ to $\mathcal{H}_1$. It is then easy to see that we can write

$$T_0(z) = \frac{V_0}{1 - V_0 G_0(z)} \equiv T_1(z) = \frac{V_1(z)}{1 - V_1(z)\left[G_0(z) - \delta G_0(z)\right]} \quad (80)$$

where we have $$V_1(z) = \frac{V_0}{1 - V_0\, \delta G_0(z)} \quad (81)$$

ie., we have ejected $T_0(z)$ defined in $\mathcal{H}_0$ with $T_1(z)$ defined in $\mathcal{H}_1$, but where we now have a new effective interaction $V_1(z)$. Writing out (80) and (81) explicitly, we have

$$T_1(z) = \frac{V_1(z)}{1 - V_1(z) \sum_{k \in D_1} \frac{1}{z - \epsilon_k}} \equiv \frac{V_1(z)}{1 - V_1(z) \int_{-D_1}^{D_1} d\epsilon \, \frac{N(\epsilon)}{z-\epsilon}} \quad (82)$$

where

$$V_1(z) = \frac{V_0}{1 - V_0 \sum_{k \in D_0 - D_1} \frac{1}{z - \epsilon_k}} \equiv \frac{V_0}{1 - V_0 \left(\int_{-D_0}^{-D_1} d\epsilon + \int_{D_1}^{D_0} d\epsilon \right) \frac{N(\epsilon)}{z-\epsilon}} \quad (83)$$

That $T_0(z) = T_1(z)$, in the energy range $-D_1 < z < D_1$, is absolutely required,

because $T(z)$ is a physical quantity. We note that the new effective interaction $V_1(z)$ is now energy-dependent. It is useful to look at this diagrammatically. We can show this as follows:

so that $V_1(z)$ involves propagation of $\delta G_0(z)$ between scattering events.

Now we can write down what are the new effective Hamiltonians for this system. We have

$$\hat{H}_0 = \sum_{k\in D_0} (\epsilon_k^0 + V_0)\, c_k^+ c_k \equiv \sum_k (\epsilon_k^0 + V_0)\, c_k^+ c_k\, \theta(D_0^2 - \epsilon_k^2)$$

$$\hat{H}_1 = \sum_{k\in D_1} (\epsilon_k^0 + V_1(\epsilon_k))\, c_k^+ c_k \equiv \sum_k (\epsilon_k^0 + V_1(\epsilon_k))\, c_k^+ c_k\, \theta(D_1^2 - \epsilon_k^2) \qquad (85)$$

and so on.

Let us now make a number of remarks on all of this, as follows.

(i) It is useful to redraw the graphs shown previously for the new $T_1(z)$, etc., after RESCALING the bandwidth back to its original value. We do this here for the realistic band we showed earlier:

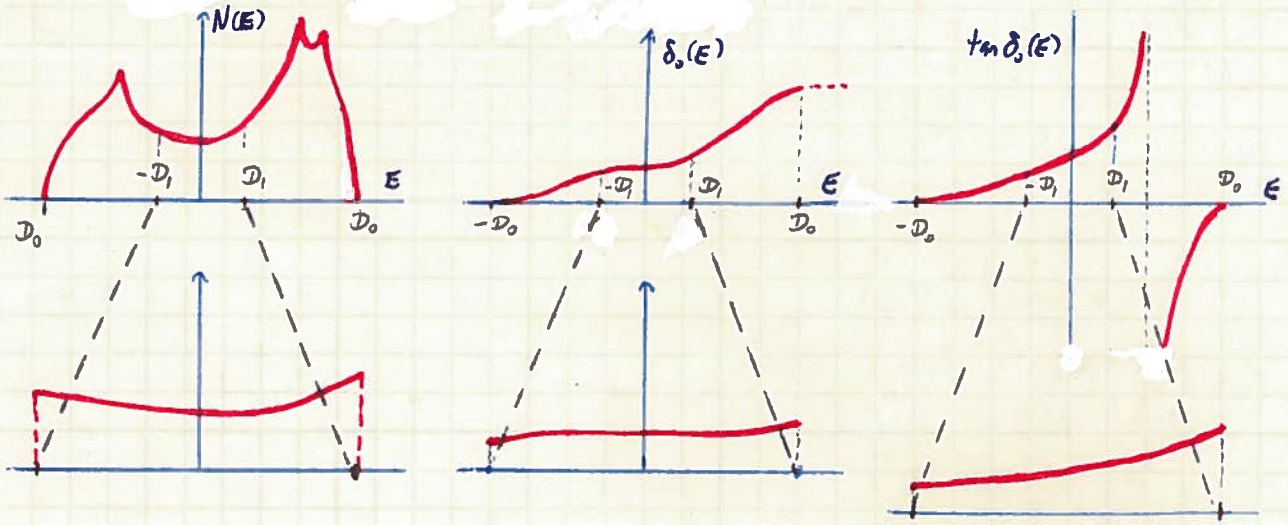

We see that the result of rescaling (to a new frequency $z_1 = D_0 z/D_1$) is to "flatten" everything out.

(ii) As we continue to reduce the D_n, we eventually get to such a narrow bandwidth that everything stops changing. We say then that we have reached a "fixed point" of the scaling: this means that we have a final

effective Hamiltonian $\mathcal{H}^*$ and a final scattering matrix $^*(z)$ given by

$$\mathcal{H}^* = \sum_{k\in D^*} (\epsilon_k + V^*)\, c_k^\dagger c_k = \sum_k (\epsilon_k + V^*)\, c_k^\dagger c_k\ \theta(D_*^2 - \epsilon_k^2) \tag{86}$$

with

$$V^*(z) = \frac{1}{\pi N_0} \tan\delta_0(0)\ \frac{1}{1 - \frac{1}{\pi}\tan\delta_0(0)\ \ln\left|\frac{D_* - z}{D_* + z}\right|} \tag{87}$$

in which everything is written in terms of $\delta_0(0)$, the phase shift as $E \to 0$, and D_*, the final cut-off, which we can now take to be as small as we like, since nothing changes anymore as we reduce D_*.

(iii) Finally, we have truncated $\hat{\mathcal{H}}$ in discrete steps. But a key feature of the procedure is that we can do this in infinitesimal steps. Suppose we write

$$V(z;\tilde{D}) = V_0(D_0) - \int_{\tilde{D}}^{D_0} dD\ \frac{dV(z;D)}{dD} \tag{88}$$

where it is obvious that for a finite difference δD, we have

$$\frac{\delta V(z)}{\delta D} = \frac{1}{\delta D}\left[\frac{V_0}{1 - V_0 \sum_{D} \frac{1}{z-\epsilon_k}} - \frac{V_0}{1 - V_0 \sum_{D-\delta D} \frac{1}{z-\epsilon_k}}\right] \tag{89}$$

where we have defined

$$\sum_{D-\delta D} \frac{1}{z-\epsilon_k} = \int_{-D}^{D} d\epsilon - \int_{-D+\delta D}^{D-\delta D} d\epsilon \left(\frac{N(\epsilon)}{z-\epsilon}\right) \tag{90}$$

Rewriting (89) as

$$\frac{\delta V(z;D)}{\delta D} = -V^2(z;D)\ \frac{\delta G_0(z;D)}{\delta D} \tag{91}$$

where

$$\left.\begin{aligned} \delta G_0(z;D) &= \sum_{k\in D} \frac{1}{z-\epsilon_k} - \sum_{k\in D-\delta D} \frac{1}{z-\epsilon_k} \\ &= \left(\frac{N(D)}{z-D} + \frac{N(-D)}{z+D}\right)\delta D \end{aligned}\right\} \tag{92}$$

The most interesting question we can ask here is how $V(z;D)$ scales when $z=0$, ie., for the lowest energy states. The differential eqtn. in (88) then becomes very simple; we have

$$\frac{\delta V(z;\mathcal{D})}{\delta \mathcal{D}} \xrightarrow[z\to 0]{} (N(\mathcal{D}) - N(-\mathcal{D}))\,\frac{V^2(\mathcal{D})}{\mathcal{D}} \qquad (93)$$

from which we get, using (88), then

$$V(\mathcal{D}) = V_0 + \int_{\mathcal{D}}^{\mathcal{D}_0} \frac{d\mathcal{D}'}{\mathcal{D}'}\,(N(\mathcal{D}) - N(-\mathcal{D}))\,V^2(\mathcal{D}) \qquad (94)$$

from which we notice that if $N(\mathcal{D}) = N(-\mathcal{D})$ (ie., a band structure which is symmetric around $\epsilon = 0$), the effective interaction does not scale at all, ie., $V(\mathcal{D}) = V_0$ for all $\mathcal{D}$.

Now (94) is a very simple example of a RG flow eqtn; these are one of the main tools in the field.

(ii) BEREZINSKII / KOSTERLITZ-THOULESS PHYSICS

We now turn to a topic which will give us a much more detailed insight into the use of RG techniques. We look at the model developed by Berezinskii, and by Kosterlitz & Thouless*, in the period 1971-74. Their results have had a huge impact on physics, for several reasons. One is that the BKT results describe a large variety of physical systems. Another is that they capture very simply the way in which topological solitons can be involved in the physics of phase transitions, with quite dramatic effects - indeed, our understanding of phase transitions was changed in a fundamental way by these results.

Some of the physical systems to which the BKT results apply include:

(a) Classical Systems (2+1-dimensions, finite T): examples are

- 2-d superfluids, superconducting fields
- 2-d easy plane spin systems (ferromagnetic or antiferromagnetic); XY-model.
- 2-d Coulomb gas
- 2-d lattice solids
- 2-d solid surfaces. and many others...

In all of these systems, one has a combination of 2 kinds of

---

* V.L. Berezinskii, JETP 32, 493 (1971), and JETP 34, 610 (1972); J.M. Kosterlitz, D.J. Thouless, J. Phys. C6, 1181 (1978); and J.M. Kosterlitz, J. Phys. C7, 1046 (1974).

excitation; a set of extended "collective mode" excitations, and a set of localized excitations (vortices in superfluids, superconductors, and XY magnets; defects or dislocations in 2-d lattices or solid surfaces, electric charges in the 2-d Coulomb gas).

(b) Quantum Systems (1+1-dimensions, $T=0$); examples are

1-d quantum spin chains
1+1-d quantum Sine-Gordon model / massive Thirring model
Kondo model
Hopping particle coupled to dissipative Ohmic bath
and many others....

In what follows I will focus on a classical example, and then discuss how the model can be mapped to other models, both classical and quantum.

2-d PHASE TRANSITIONS: There is a very old argument (originally formulated by Peierls) which is supposed to show that long-range order cannot exist in a 2-dimensional system, unless there is some long-range coupling which can enforce it. If true this theorem would show that there could be no solid-liquid transition in 2d, nor a superfluid-normal fluid transition.

The argument runs as follows. Consider what would happen if, eg., we had a 2-d crystal. Then we could define lattice phonons, with amplitude

$$\underline{u}_j = \sum_{\underline{q}} \underline{u}_{\underline{q}} e^{i\underline{q}\cdot\underline{r}_j} \tag{95}$$

on site j at position $\underline{r}_j$; the vector $\underline{u}_{\underline{q}}$ is then the phonon amplitude for wave-vector $\underline{q}$. At low energy we deal with acoustic phonons, with dispersion relation $\omega_q^\alpha \sim c_\alpha q$, where $\alpha = \perp, \parallel$ labels longitudinal & transverse modes.

Now, for our system, we expect equipartition of energy to hold between the modes, which at temperature T, in the classical regime, implies that

$$\langle \underline{u}_{\underline{q}}\, \underline{u}_{-\underline{q}} \rangle \propto kT/m\omega_q^2 \tag{96}$$

and Fourier transforming, we have

$$\left.\begin{aligned} \langle |\underline{u}_i - \underline{u}_j|^2 \rangle &= \frac{kT}{m} \iint_{B.Zone} dq_x\, dq_y\, \frac{\cos[q_x(r_i^x - r_j^x)] + \cos[q_y(r_i^y - r_j^y)]}{\omega_q^2} \\ &\sim \frac{kT}{m} \int_{1/R_{ij}}^{1/a_0} \frac{q\,dq}{\omega_q^2} \sim 2\frac{kT}{mc_0^2} \ln\left|\frac{R_{ij}}{a_0}\right| \end{aligned}\right\} \tag{97}$$

where $R_{ij} = |\underline{r}_i - \underline{r}_j|$ is the distance between sites i and j, and a_0 is a lattice spacing.

We see that the fluctuations away from a lattice structure diverge logarithmically for widely separated sites, indicating a lack of long-range crystalline order. Two obvious questions arise here:

(i) What if there is a gap in the low-energy spectrum? This is hard to arrange for phonons, but in the example of magnetic systems (where the same argument as above goes through, this time with spin fluctuations having RMS amplitude $\langle S_q S_{-q} \rangle$), one can arrange a gap, ie, one can have a magnon spectrum of form

$$\omega_q^2 = \Delta_0^2 + c^2 q^2 \qquad (98)$$

with a gap Δ_0 which can arise, eg., if one has long-range dipolar interactions between the spins. The gap then suppresses the logarithmic divergence.

(ii) What causes the large fluctuations — or, to put it another way, what kind of excitations are involved? We can get a quick idea of this by considering how a 2-d lattice might distort at long distances. The figure shows 2 ways this can happen:

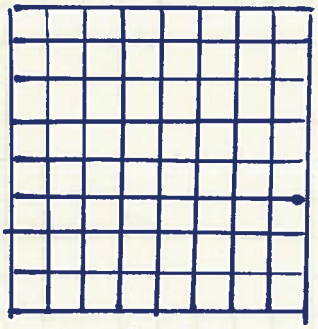

ORDERED 2-D

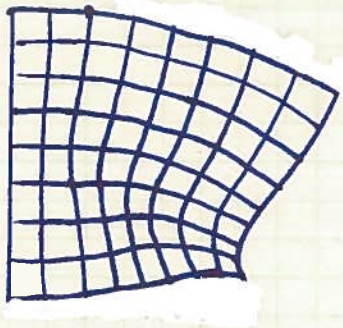

SOFT FLUCTUATIONS

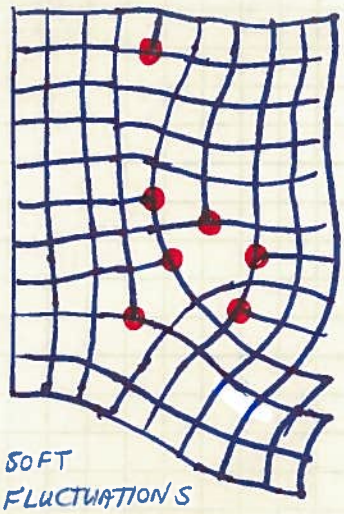

SOFT FLUCTUATIONS PLUS DEFECTS

The easiest way to deform the ordered 2-d lattice is via long-wavelength slow fluctuations - these are basically phonons, which we can call "soft" (ie, low energy) phonons.

There is another way to deform the lattice, which costs more energy; this involves inserting defects or dislocations into the lattice structure - these are strong local deformations of the system.

The effect of the 2 kinds of deformation is quite different. The soft fluctuations do not change the order locally, or destroy the crystalline order locally. One sees intuitively that the system becomes a little "floppier", or more labile, but it is still capable of resisting shear

forces. On the other hand the effect of the defects is to destroy order at the local level; and as we will see, it also reduces the shear resistance to zero, so that the system is no longer solid.

2-d SUPERFLUIDS : We can get an alternative perspective on all of this by looking at how the same physics emerges for a 2-d superfluid. We can describe the superfluid locally by a local order parameter

$$\psi(\underline{r},t) = \psi_0(\underline{r},t)\, e^{i\phi(\underline{r},t)} \tag{98}$$

where $\psi_0(r,t)$ is supposed to be slowly-varying in space & time, whereas $\phi(r,t)$ can vary rapidly; the superfluid velocity is defined as

$$\underline{v}_s(\underline{r},t) = \frac{\hbar}{m}\underline{\nabla}\phi(r,t) \tag{99}$$

This is just like classical hydrodynamics for an incompressible ideal fluid in 2 dimensions, except that we allow for the superfluid density to vary with position; we have

$$\rho_s^0(\underline{r},t) = |\psi(r,t)|^2 = |\psi_0(r,t)|^2 \tag{100}$$

However, this density only varies appreciably near the vortex core, where it goes to zero. For an isolated vortex, or near a vortex core, we have

$$\underline{v}_s(r) \sim (\hat{z}\times\hat{r})\frac{\hbar}{m} q \frac{1}{|\underline{r}|} \tag{101}$$

where q is the "vortex charge"; stable vortices have $q = \pm 1$.

As you will note, the system of vortices is completely isomorphic in 2 dimensions to a set of electric charges; lines of constant superfluid phase correspond to electric field lines in the charge system; superfluid flow lines correspond to equipotentials in the charge system. We will return to the system of charges later. We note also that both of these systems can also be described by some meromorphic function in the complex plane, of form

$$f(z) = \sum_j \frac{q_j}{z - z_j} + f_0(z) \tag{102}$$

where $f_0(z)$ is analytic in the domain of interest (i.e., it is "source free"); the "charges" or vortex cores are at points z_j.

Finally, note that the energy of an isolated vortex in some region of size R is given by

$$E = \tfrac{1}{2}\rho_s^0 \int d^2r\, v_s^2(\underline{r}) \sim \frac{\pi\hbar^2}{m^2} q^2 \rho_s^0 \int_{a_0}^{R} \frac{r\,dr}{r^2} \sim \frac{\pi\hbar^2}{m^2} q^2 \rho_s^0 \ln\left|\frac{R}{a_0}\right| \tag{103}$$

where we simply integrate over the kinetic energy of the superfluid.

Let us now make a division between the "regular" part of $\underline{v}_s(\underline{r},t)$, unconnected with vortices, and that part coming from the vortices - in the same way we divided $f(z)$ between its regular analytic part $f_0(z)$ and that part sourced by the poles; we write

$$v_s(\underline{r}) = \frac{\hbar}{m}\left\{\nabla\phi_0(\underline{r}) + 2\pi(\hat{\underline{z}}\times\underline{\nabla}_r)\int d^2r'\, G_v(r,r')\, q(r')\right\} \tag{104}$$

where $G_v(r,r')$ is the Green function for the superflow field, defined by

$$\nabla_r^2 G(\underline{r},\underline{r}') = \delta(r-r') \tag{105}$$

in the domain of interest, and $q(r)$ defines the "vortex field"; one has

$$q(r) = \sum_j q_j\,\delta(\underline{r}-\underline{r}_j) \tag{106}$$

where the $\{q_j\}$ are the relevant charges. The solution to (105) in an unbounded domain is just

$$G_v(r,r') = \frac{1}{2\pi}\ln\left|\frac{\underline{r}-\underline{r}'}{a_0}\right| + C(a_0) \tag{107}$$

where a_0 is a regularization parameter (amounting essentially to a UV momentum cut-off), and $C(a_0)$ a constant of integration.

The division made in (104) now allows us to treat the statistical mechanics of the 2-d superfluid. Recalling that we are interested in the classical theory, we note that the partition function / generating functional of our system can be written as

$$\mathcal{Z} \sim \int \mathcal{D}\phi(r,t)\, e^{-\beta\mathcal{H}[\phi]} \tag{108}$$

where we have no external "source field" coupling to $\phi(\underline{r},t)$; the Hamiltonian is just

$$\mathcal{H} = \tfrac{1}{2}\rho_s\int d^2r\, v_s^2(\underline{r}) \tag{109}$$

which we write in the form $\mathcal{H} = \mathcal{H}_0 + \mathcal{H}_V$, with

$$\beta\mathcal{H}_0 = \tfrac{1}{2}K_0\int d^2r\,(\nabla\phi_0(r))^2 \tag{110}$$

where we define

$$K_0 = \frac{\hbar^2}{m^2kT}\rho_s^0(T) \tag{111}$$

in which $\rho_s^0(T)$ is the "bare" superfluid density, computed without vortices, and where

we have

$$\left.\begin{aligned}\beta H_V &= 2\pi^2 K_0 \int d^2r \int d^2r_1 \int d^2r_2 \; \nabla_r G_V(r,r_1)\, q(r_1) \cdot \nabla_r G_V(r,r_2)\, q(r_2) \\ &= -\pi K_0 \int d^2r \int d^2r' \; q(r) q(r') \ln\left|\frac{r-r'}{a_0}\right| + \frac{\mu(T)}{kT}\int d^2r\, q^2(r)\end{aligned}\right\} \quad (112)$$

where we absorb the various constants involved in the definition of the "self-interaction" term $\int d^2r\, q^2(r)$ into a chemical potential $\mu(T)$, recognizing that $\mu(T)$ gives us the energy required to create a vortex, of charge q. We can also write

$$\beta H_V = -\pi K_0 \sum_{i\neq j}\sum q_i q_j \ln\left|\frac{r_i - r_j}{a_0}\right| + \beta\mu(T)\sum_j q_j^2 \quad (113)$$

The partition function can now be written in the form we want, as a trace over 2 separate sets of variables, as

$$\boxed{\begin{aligned} Z &= Tr\, e^{-\beta(H_0 + H_V)} \\ &= Tr\, \exp\left\{ K_0\left[\tfrac{1}{2}\int d^2r\,(\nabla\phi)^2 - \pi \sum_{i\neq j}\sum q_i q_j \ln\left|\frac{r_i - r_j}{a_0}\right|\right] + \beta\mu\sum_j q_j^2 \right\} \quad (114) \\ Tr &\equiv \int \mathcal{D}\phi_0(r,t) \sum_{n=0}^{\infty}\left(\frac{1}{n!}\right)^2 \int_{D_0} d^2r_1 \cdots d^2r_{2n} \end{aligned}}$$

Before we analyze this partition function using RG theory, let's note several key points about this partition function, some of which have quite broad implications. In particular

(i) It is immediately obvious how one could have derived the same form for $\mathcal{H} = H_0 + H_V$ for many other systems. Thus, eg., consider the "Coulomb gas" problem, of a set of positive and negative charges (of magnitude $q_j = \pm 1$), which interact in the 2-d plane. We can consider 2 cases - either the charges move in a 2-d vacuum, and have fixed numbers n_+, n_-; or we deal with some neutral medium, described by a field $\phi_0(r)$, from which charges can be excited in equal numbers of positive and negative sign. In either case we have an electric field

$$E(r,t) = E_0(r,t) + (\hat{z}\times\nabla_r)\int d^2r'\, G_p(r,r')\, q(r',t) \quad (115)$$

where $E_0(r,t)$ is either some external field (in the vacuum case) or some internal divergence-free field generated by the polarizable neutral medium. This equation is precisely analogous to (104) for the superflow velocity; in the vacuum case we

have a partition function

$$Z = \int d\underline{r}_1 \cdots d\underline{r}_{2n} \exp\left\{ \frac{K_0}{2} \sum_{i \neq j} \sum q_i q_j \ln\left|\frac{\underline{r}_i - \underline{r}_j}{a_0}\right| + \beta\mu(T) \sum_j q_j^2 \right\} \tag{116}$$

whereas in the latter case we have precisely (114), except that now $K_0 = \beta\varepsilon_0^{-1}$. One can also generalize to the case where we have a different number of possible charges, i.e., where in the medium $n_+ \neq n_-$; in this case the Tr in (114) is replaced by

$$Tr \rightarrow \int \mathcal{D}\phi_0(\underline{r},t) \sum_{n_+=0}^{\infty} \sum_{n_-=0}^{\infty} \frac{1}{n_+!} \frac{1}{n_-!} \int_{D_0} d\underline{r}_1^2 \cdots d\underline{r}_{n_+}^2 \int_{D_0} d\underline{r}_1'^2 \cdots d\underline{r}_{n_-}'^2 \tag{117}$$

but otherwise everything is as before. Other models of interest here include the XY spin model, for which one has the vortex interaction Hamiltonian

$$\beta H_V = -\pi K_0 \sum_{i \neq j} \sum p_i p_j \ln\left|\frac{\underline{r}_i - \underline{r}_j}{a_0}\right| + \beta\mu(T) \sum_j p_j^2 \tag{118}$$

where $p_j = \pm$ is the polarization of the XY vortex for the spins. One can generalize such models to include anisotropy in the plane, etc., to produce a variety of fascinating physics (discussed later).

(ii) A key feature of our results is that there is no "cross term" in the Hamiltonian $\mathcal{H}$, involving an integration over $\nabla\phi_0(r)$ and $G_V(r-r')q(r')$. For the superfluid this can be understood physically in the same way as we understand any soliton problem (the Sine-Gordon case being particularly transparent); there can be no interaction between the soliton and small fluctuations around the soliton configuration that are linear in the fluctuations, because the soliton configuration is already a minimum action solution to the eqtns of motion. Thus any such term must integrate to zero; the phase field $\phi_0(r)$ must adjust itself to the positions $\{\underline{r}_j\}$ of the vortices to make this so. The same will apply to all of the systems we deal with.

(iii) The parameter a_0, introduced as a UV momentum cutoff, also eliminates the singularity in "charge density" for the Coulomb gas system at the positions of the charges, or the singularity in "flux density" at the vortex core. Otherwise we would have

$$\nabla^2\phi(r) = -2\pi \frac{\hbar}{m} q_j \delta(\underline{r} - \underline{r}_j) \tag{119}$$

for each vortex of charge q_j, and the analogous Poisson eqtn for electric charges in the Coulomb gas case. Essentially we now smear charge, or vorticity/flux density, over a disc of radius a_0 centred at $\underline{r}_j$. The restriction $\int_{D_0} d\underline{r}_j^2$ simply means $\int d\underline{r}_j^2\, \theta(|\underline{r} - \underline{r}_j| - a_0)$.

I stress here that the theory used here for the description of the 2-d superfluid is in some ways quite primitive – it is a classical theory (in that $\underline{v}_s$ and ρ_s are just numbers, and we ignore quantum fluctuations; the phase field $\phi(\underline{r},t)$ and its conjugate density field $\rho(\underline{r})$ are treated as c-number functions). Even within

this simple description, a proper discussion would look at the way in which the function K_0 (and it's renormalized version $K(T)$) is related to the transverse current-current correlation function — we return to this briefly below.

With all this in mind, we now turn to the KT scaling theory.

KT SCALING THEORY : The striking result, which we will derive here, that comes out of a scaling treatment of the effective Hamiltonian derived above, is a new kind of phase transition in the system, involving a binding/unbinding of vortices (in the superfluid) or charges (in the Coulomb gas. Before we go into the details, it is useful to understand both why the existence of a phase transition follows from elementary arguments, and why it is nevertheless of profound significance.

Consider a set of vortices or charges in a 2-dimensional domain of size L^2. We can estimate the free energy $F = E - TS$ of a single charge in the system very simply; we have

$$\left.\begin{aligned} F &\sim E_0 \ln\left|\frac{L}{a_0}\right| - T\left(k \ln\left|\frac{L^2}{a_0^2}\right|\right) \\ &= (E_0 - 2kT) \ln\left|\frac{L}{a_0}\right| \end{aligned}\right\} \text{ single charge} \qquad (120)$$

where the result for E comes from (103), so that $E_0 = \pi(\hbar^2/m^2)\rho_s$ for a single vortex, and the result for $S = k \ln W$ comes from estimating the number of different vortex configurations by dividing the 2-d plane, of area L^2, into elementary cells of area a_0^2. We therefore expect a phase transition at a temperature $T_K \sim E_0/2k$, between a high-T phase where vortices proliferate, and a low-T phase where they are absent. If we generalize this argument to $2n$ non-interacting vortices, it goes through in the same way — we just get

$$F \sim n(E_0 - 2kT) \ln\left|\frac{L}{a_0}\right| \qquad n \text{ non-interacting charges} \qquad (121)$$

However the problems begin once we take account of inter-charge/inter-vortex interactions. This is what the scaling is intended to deal with.

At first glance this seems like just another phase transition. However what is fascinating and illuminating here is that there is no apparent appearance or disappearance of any order parameter here. Thus in the superfluid case, we still have a local order parameter $\psi(r,t) = \psi_0(r,t)\, e^{i\phi(r,t)}$ defined everywhere except for the vortex cores; in the case of a 2-d lattice solid, lattice order appears local except at the defects. Thus it was necessary to invent a new kind of phase transition, accompanied by the appearance of a new kind of order, called "topological order"; more of this below.

How can we deal with vortex interactions in the calculation of the free energy? The key insight of Kosterlitz & Thouless was to observe that the quantity $K_0(T)$, defined by (111), is just the bare version of a superfluid "dielectric function", describing the response of the system to perturbations of the superfluid; for the Coulomb gas K_0 refers to the bare dielectric function ε_0. The effect of allowing vortex or charge interactions will be, amongst other things, to allow screening to take place:

the effect of both the phase fluctuation in $\phi_0(r)$, and the appearance of vortices in between some given pair of vortices, will partially screen the interaction between this pair. Thus we expect $K_0(T)$ to scale, ie., to change once interactions are introduced, and to change with temperature.

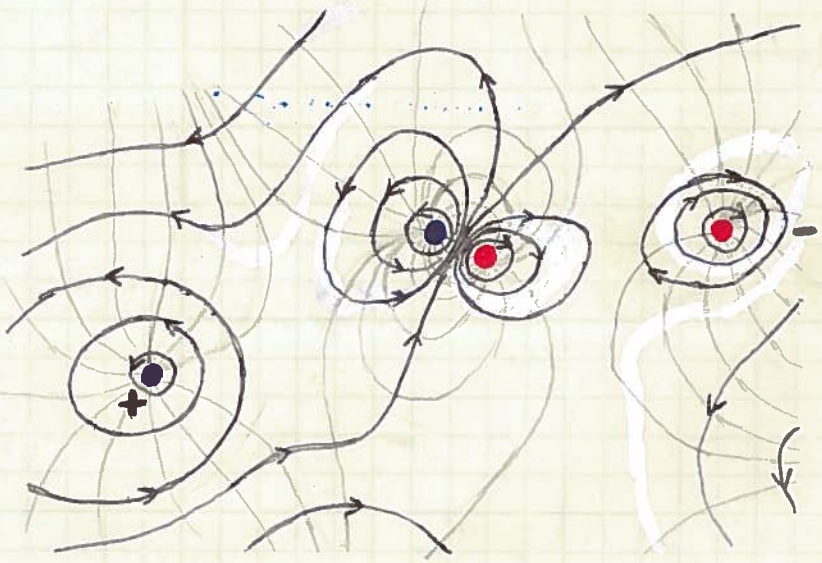

To see the kind of thing that happens, the figure shows a configuration of 4 vortices. The two distant vortices, of opposite sign, have the flow field between them distorted by the presence of a "dipolar pair" of vortices.

In the Coulomb gas, the region between the 2 distant charges has an electric field distorted by the presence of a dipolar charge pair.

Now the key point here is that the intermediate region now has become strongly polarizable - the dipolar pair can be polarized by the field of the 2 distant charges. This modifies the interaction between the 2 charges, as well as modifying the flow field / electric field.

To see how this affects things, the idea of the RG is, instead of trying a brute-force calculation of the renormalized interaction, one does this in increments, just as we did in energy space for the renormalized scattering. Here we will do this in real space - the analogue of removing increments at high energies (UV energy cutoff) is to progressively "coarse-grain" the real space description of the system (IR real-space cutoff). To see what this means, we look at the above picture after coarse-graining has been accomplished. The intervening dipolar pair has been eliminated, because the separation between the vortices was smaller than the new short-distance cutoff - all that is left is a strong dipolar fluctuation. For the 2 pictures to be equivalent (the fine-grained and the coarse-grained one), it is clear that the coarse-grained medium and the fine-grained medium must be different - they will have different polarizabilities and fluctuation spectra. If we continue the coarse-graining, we will be left only with the 2 charges of the distant pair, with no obvious difference except that the flow pattern has been "weakened"; the interaction between the 2 distant vortices is thus renormalized.

We now need to implement these ideas formally. The coarse-graining is accomplished by changing the domain of integration - we go from $\int_{D_0} d^2r_j$ to $\int_{D_1} d^2r_j$, where the domain D_1 is

defined by $\int_{D_1} d^2\underline{r}\ \theta(|\underline{r}-\underline{r}_j| - a_1^2)$, where $a_1 > a_0$. The basic idea of the derivation involves 2 steps:

(I) We assume we are near the binding/unbinding transition, so that the concentration of vortices is small (we will see below how to implement this idea practically); we then calculate the renormalized interaction between the 2 distant vortices caused by a single intervening vortex pair

(II) We then implement a RG scaling procedure, gradually scaling out the short wavelength modes to end up with a long-wavelength effective action for dilute interacting vortex pairs described by scaling laws for the 2 key physical quantities, these being the renormalized superfluid density and the renormalized vortex chemical potential.

STEP 1 : RENORMALIZED INTERACTION : I will describe 2 different ways of calculating the renormalized interaction - this is done to give a better intuitive feeling for what is going on. In both cases we will start off from an unrenormalized interaction between 2 vortices that we write in the form

$$\beta V_0(\underline{r}_i - \underline{r}_j) = \beta V_{ij}^0 = \pi K_0 q_1 q_2 \ln\left|\frac{\underline{r}_i - \underline{r}_j}{a_0}\right| \equiv W_{ij}^{(0)} \qquad (122)$$

This will be the input into our theory — it, along with the bare chemical potential μ_0, will describe the bare theory.

METHOD 1 : The first way we will do this is by straightforward calculation; it is a little unwieldy, but has the advantage of displaying the physics in a clear intuitive way.

Consider the situation shown in the figure - we have a widely separated vortex pair, with vortices of opposite charge at position $\underline{r}_i$ and $\underline{r}_j$, and with an intermediate dipole pair of vortices at positions $\underline{s}_1$ and $\underline{s}_2$. We also define

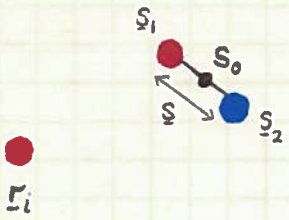

$$\underline{s}_0 = \tfrac{1}{2}(\underline{s}_1 + \underline{s}_2)$$
$$\underline{s} = \tfrac{1}{2}(\underline{s}_1 - \underline{s}_2) \qquad (122)$$

Now we are going to assume that the vortices are dilute — the "dilute gas approx." This means that we can consider what follows as an expansion in powers of the "fugacity" $y = e^{-\beta\mu(T)}$; we assume that

$$y_0(T) = e^{-\beta\mu_0(T)} \ll 1. \qquad (123)$$

We can then write the renormalized effective interaction between vortices at $\underline{r}_i$ and $\underline{r}_j$ as an expansion in powers of this fugacity, taking account only of a single intervening vortex pair between these 2 vortices. Formally this means that we write.

$$e^{-\beta V_{ij}} \equiv e^{-W_{ij}} = e^{-W_{ij}^{(0)}}\left[\frac{1 + y_0^2 \int ds_1^2 \int ds_2^2\, e^{-W_{ij}^{(2)}(s_1,s_2)} + O(y_0^4)}{1 + y_0^2 \int ds_1^2 \int ds_2^2\, e^{-W_{s_1 s_2}^{(0)}} + O(y_0^4)}\right] \qquad (124)$$

where

$$W_{ij}^{(2)}(s_1,s_2) = \beta\left[V^0(s_1-s_2) + \left(V^0(r_i-s_1) + V^0(r_j'-s_2) - V^0(r_i-s_2) - V^0(r_j'-s_1)\right)\right] \qquad (125)$$

and

$$W^0_{(s_1,s_2)} = \beta V^0_{(s_1-s_2)} \qquad (126)$$

The numerator in (124) is just the sum of all the interactions in the 4-vortex system, exponentiated to give the free energy; and the denominator is a normalising factor, since we are expanding a partition function here.

We then note that because the interaction between the charges in the intermediate dipole is strongest at short ranges, fluctuations with widely separated pairs are unlikely (indeed the probability goes like $e^{-\beta\pi K_0 \ln|r_i-r_j'/a_0|}$, ie., like $((r_i-r_j')/a_0)^{-\pi\beta K_0}$), so we should assume that $|s_1-s_2| \ll |r_i-r_j'|$. We then rewrite all the coordinates in (125) and (126) in terms of S_0 and s, and expand in powers of $|s|$ to get

$$W_{ij}^{(2)}(s_1,s_2) = \beta\left[V^0(s) + \left(s\cdot\nabla_{S_0} V^0(r_j-S_0) - s\cdot\nabla_{S_0} V^0(r_i-S_0)\right) + O(s^3)\right] \qquad (127)$$

so that we get

$$e^{-\beta V_{ij}} = e^{-\beta V_{ij}^0}\left\{1 + y_0^2 \int d^2S_0 \int_{D_0} ds^2\, e^{-\beta V^0(s)}\left[\pi K_0\, s\cdot\nabla_{S_0}\left(V^0(r_j-S_0) - V^0(r_i-S_0)\right) + 2\pi^2 K_0^2\left(s\cdot\nabla_{S_0}\left(V(r_j-S_0) - V(r_i-S_0)\right)\right)^2\right]\right\} \qquad (128)$$

plus terms $\infty O(y_0^4)$. If we now do the angular integrations in (128), and integrate by parts, we get the result

$$e^{-\beta V_{ij}} = \exp\left\{-\beta\left[V_{ij}^0\left(1 + \frac{4\pi^3}{a_0} y_0^2 K_0^2 V_{ij} \int_{D_0} ds\, s^3\, e^{-2\pi K_0 \ln|s/a_0|}\right) + O(y_0^4)\right]\right\} \qquad (129)$$

which then allows us to write

$$e^{-\beta V_{ij}} = e^{-\pi \tilde{K}(T)\, q_i q_j \ln\left|\frac{r_i-r_j}{a_0}\right|} \qquad (130)$$

where

$$\tilde{K}(T) = K_0 - 4\pi^3 K_0^2 y_0^2 a_0^{2\pi K_0 - 1} \int_{a_0}^{\infty} ds\, s^{3-2\pi K_0} + O(y_0^4) \qquad (131)$$

This is our first way of getting the result for the renormalized interaction - note that the superfluid nature of the system was not involved in this derivation at all.

METHOD 2 : The above derivation was essentially a small fugacity expansion, framed in terms of the integration over intermediate dipole fluctuations. Again at no point did we need knowledge of superfluids; we simply discussed the properties of a set of interacting charges in 2 dimensions. We now look explicitly at a 2-d superfluid.

We begin by considering the current-current response function for a fluid. We write

$$\chi_{\mu\nu}(x,x') = \langle J_\mu(x) J_\nu(x') \rangle \tag{132}$$

in spacetime coordinates - the various components of this are, in non-relativistic notation:

$$\left.\begin{aligned} \chi_{00}(\underline{r},t) &= \langle \rho(\underline{r},t)\rho(0,0)\rangle \\ \chi_{0j}(\underline{r},t) &= \langle \rho(\underline{r},t)\, J_j(0,0)\rangle \end{aligned}\right| \quad \left.\begin{aligned} \chi_{ij}(\underline{r},t) &= \langle J_i(\underline{r},t)\, J_j(0,0)\rangle \\ &\equiv \chi_{ij}^{JJ}(\underline{r},t) \end{aligned}\right\} \tag{133}$$

where $\underline{J}(\underline{r},t)_N$ is the 3-current; in a neutral fluid this is just the mass current, ie., $\underline{J}(\underline{r},t) = \sum_{j=1} m_j \underline{v}_j(\underline{r},t)$.

Before beginning, we first recall some key results for the response function $\chi_{ij}^{JJ}(\underline{k},\omega)$, the Fourier transform of $\chi_{ij}^{JJ}(\underline{r},t)$, for a uniform system. We can separate this response function into 2 components — this is typically done in 2 different ways, viz.,

$$\left.\begin{aligned} \chi_{ij}^{JJ}(\underline{k},\omega) &= \chi^L(\underline{k},\omega)\hat{k}_i\hat{k}_j + \chi^T(\underline{q},\omega)\left[\delta_{ij} - \hat{k}_i\hat{k}_j\right] \\ &\equiv \chi''(\underline{k},\omega)\,\delta_{ij} + \chi^\perp(\underline{k},\omega)\,\hat{k}_i\hat{k}_j \\ &\equiv \chi^T(\underline{k},\omega)\,\delta_{ij} + \left(\chi^L(\underline{k},\omega) - \chi^T(\underline{k},\omega)\right)\hat{k}_i\hat{k}_j \end{aligned}\right\} \tag{134}$$

where χ^L, χ^T refer to "longitudinal" and "transverse" components, and χ'', $\chi^\perp$ refer to "parallel" and "perpendicular" components. We then have the following results:

Normal Fluid : Any fluid will have normal and superfluid components, as shown by Landau. For the normal component we have

$$\left.\begin{aligned} &\chi_{ij}^{JJ}(\underline{k},\omega) \xrightarrow[\text{Normal}]{} \chi_N(\underline{k},\omega)\,\delta_{ij} \\ &\text{with} \quad \chi_N(\underline{k},\omega) = \chi''(\underline{k},\omega) = \chi^T(\underline{k},\omega) \end{aligned}\right\} \tag{135}$$

The normal fluid density is then given, in the homogeneous case, by

$$\rho_n = \lim_{|\underline{k}|\to 0} \chi_N(\underline{k},0) \equiv \lim_{|\underline{k}|\to 0} \int \frac{d\omega}{\pi}\,\frac{1}{\omega}\,\mathrm{Im}\,\chi_N(\underline{k},\omega) \tag{136}$$

Superfluid : for the superfluid we have

$$\left.\begin{aligned} &\chi_{ij}^{JJ}(\underline{k},\omega) \xrightarrow[\text{superfluid}]{} \chi_S(\underline{k},\omega)\,\hat{k}_i\hat{k}_j \\ &\text{with} \quad \chi_S(\underline{k},\omega) = \chi^\perp(\underline{k},\omega) \equiv \left(\chi^L(\underline{k},\omega) - \chi^T(\underline{k},\omega)\right) \end{aligned}\right\} \tag{137}$$

and so the superfluid density is given by

$$\rho_s = \lim_{|\underline{k}|\to 0} \chi_S(\underline{k},0) \equiv \lim_{|\underline{k}|\to 0} \int \frac{d\omega}{\pi} \frac{1}{\omega} \mathrm{Im}\, \chi_s(\underline{k},\omega) \tag{138}$$

In eqtns (136) and (138) we use Cauchy's thm., viz., that $\chi(z) = \int \frac{d\omega}{\pi} \frac{\mathrm{Im}\,\chi(\omega)}{\omega - z}$ (139)

The total fluid response is the sum of the normal & superfluid responses, ie., we have a total response given by (134), and $\rho = \rho_N + \rho_s$.

In a superfluid or a Bose-condensed system we have the same problem as we noted above for a 2-d solid, viz., that long-wavelength fluctuations destroy long-range order, so that ρ_s as defined in (138) is suppressed to zero at any finite T, when dimensionality $D = 2$. However this does not destroy short-range order, as we have already noted (cf eqtn (98)).

Let us return to the expression (104), which seperates out the regular and vortex components of the superfluid velocity, and insert this into our expression for the superfluid density in (138) above. We define the "superfluid stiffness" $\tilde{K}(T)$ by

$$\tilde{K}(T) = \frac{\hbar^2}{m^2 kT} \rho_s(T) \tag{140}$$

where $\rho_s(T)$ is now the fully renormalized ρ_s that is defined by the low-$\underline{k}$ limit of the response function defined in (138). We need to calculate

$$\begin{aligned} \chi_{ij}(\underline{k},0) \to \chi_s(\underline{k},0)\, \hat{k}_i \hat{k}_j \\ &= m^2 \langle v_s^i(\underline{k})\, v_s^j(-\underline{k}) \rangle \\ &= \int d^2r\, e^{i\underline{k}\cdot\underline{r}} \left\langle \left(\nabla_i \phi_0(r) + 2\pi(\hat{z}\times\nabla_i)\int d^2r' G_V(r-r') q(r')\right)\left(\nabla_j \phi_0(0) + 2\pi(z\times\nabla_j)\int d^2r' G(-r') q(\underline{r}')\right)\right\rangle \end{aligned} \tag{141}$$

The average in $\langle \ldots \rangle$ includes here an averaging over the slow field $\phi_0(\underline{r})$ as well as the vortex field $q(\underline{r})$. Carrying out the average $\int \mathcal{D}\phi_0(r) \equiv \prod_{\underline{k}} \int \mathcal{D}\phi_{\underline{k}}$, we get the expression

$$\tilde{K}(T) = K_0 - 4\pi^2 K_0^2 \lim_{\underline{k}\to 0} \frac{1}{k^2} \langle q_{\underline{k}}\, q_{-\underline{k}} \rangle \tag{142}$$

which is equiv

$$\rho_s(T) = \rho_s^0(T) - \frac{1}{kT}\left(\frac{\hbar}{m}\rho_s^0(T)\right)^2 \lim_{\underline{k}\to 0} \frac{1}{k^2} \langle q_{\underline{k}}\, q_{-\underline{k}} \rangle \tag{143}$$

where $\langle q_{\underline{k}}\, q_{-\underline{k}} \rangle$ is the momentum space vortex field correlator, ie.,

$$\langle q_{\underline{k}}\, q_{-\underline{k}} \rangle = \int d^2r\, e^{i\underline{k}\cdot\underline{r}} \langle q(\underline{r})\, q(0) \rangle \tag{144}$$

with $q(\underline{r})$ given as before by (106). Now we note that

$$\lim_{|k|\to 0} \langle q_{\underline{k}} q_{-\underline{k}} \rangle \propto k^2 \tag{145}$$

since the $k=0$ contribution to $\langle q_k q_{-k} \rangle$ (in a power series expansion in k of $\langle q_{\underline{k}} q_{-\underline{k}} \rangle$) must be zero by charge neutrality (i.e., since $\int d^2\underline{r}\, q(\underline{r}) = 0$). It then follows that

$$\langle q_{\underline{k}} q_{-\underline{k}} \rangle = \frac{\pi}{2} \int dr\, r^2 \langle q(\underline{r}) q(0) \rangle \tag{146}$$

using (144), so that we can also write, in place of (142), the result

$$\left.\begin{aligned} \tilde{K}(T) &= K_0(T) - 2\pi^2 K_0^2(T) \int_0^{2\pi} d\theta \int_{a_0}^{\infty} dr\, r^3 \langle q(\underline{r}) q(0) \rangle \\ &\equiv K_0(T) - 4\pi^3 K_0^2(T) \int_{a_0}^{\infty} dr\, r^3 \langle q(\underline{r}) q(0) \rangle \end{aligned}\right\} \tag{147}$$

Now we are almost at the previous result in (131). To get there, we again use the assumption that $y_0 \ll 1$ (note that we have not yet used this - the result in (147) is valid no matter whether we have a dilute vortex gas or not). It then follows that we can calculate $\langle q(\underline{r}) q(0) \rangle$ by looking at single vortex pairs. The energy of a single vortex pair is

$$E_{2v} = 2\mu_0 - 2\pi\beta K_0(T) \ln\left|\frac{r}{a_0}\right|$$

and the probability of finding such a pair at a distance r from each other is

$$\left.\begin{aligned} P(r)\, dr &\sim 2\pi r\, dr \left(\frac{1}{a_0^2}\right)^2 e^{-2E_v/kT} \\ &= 2\pi r\, dr\, \frac{1}{a_0^4}\, y_0^2\, r^{-2\pi K_0(T)} \end{aligned}\right\} \tag{148}$$

where we use $q(r)q(0) = 1$ (oppositely signed vortices). But (148) immediately implies that

$$\langle q(\underline{r}) q(0) \rangle = \frac{1}{a_0^4}\, y_0^2\, r^{-2\pi K_0(T)} \tag{149}$$

which gives

$$\boxed{\tilde{K}(T) = K_0(T) - 4\pi^3 y_0^2(T) K_0^2(T) \int_{a_0}^{\infty} \frac{dr}{a_0} \left(\frac{r}{a_0}\right)^{3-2\pi K_0(T)}} \tag{150}$$

which is what we found previously in (131).

So far so good. However, we now need to understand how to scale this to very long wavelengths, where there may be many vortex pairs around.

STEP 2: RG EQUATIONS & PHASE DIAGRAM : We are now in a position to carry out the same kind of rescaling operation that was done in the simple impurity problem before. The basic idea is now to do a real space renormalization of the equation (150) that we have derived for $\tilde{K}(T)$. Since we have already done this for the impurity scattering T-matrix, the procedure is very familiar.

To do the scaling, it is easiest to write things in terms of $\tilde{K}^{-1}(T)$; if we write $\tilde{K} = K_0 + \delta K$, then $\tilde{K}^{-1} = K_0 + \delta K/K_0^2 + \cdots$, so that

$$\tilde{K}^{-1}(T) = K_0^{-1}(T) + 4\pi^3 y_0^2(T) \int_{a_0}^{\infty} \frac{dr}{a_0} \left(\frac{r}{a_0}\right)^{3-2\pi K_0(T)} \tag{151}$$

which conveniently gets rid of the K_0^2 term on the RHS. Now we imagine rescaling, by increasing a_0 to $a_0(1+\delta\ell) = a_0 e^{\delta\ell}$; this will involve rescaling both $y_0(T)$ and $K_0(T)$. We begin with the rescaling of $K_0(T)$; we have

$$\tilde{K}^{-1}(T) = K_1(T) + 4\pi^3 y_0^2(T) \int_{a_1}^{\infty} \frac{dr}{a_0} \left(\frac{r}{a_0}\right)^{3-2\pi K_1(T)} \tag{152}$$

with $a_1 = a_0 e^{\delta\ell}$, and

$$K_1^{-1}(T) = K_0^{-1}(T) + 4\pi^3 y_0^2(T) \int_{a_0}^{a_0 e^{\delta\ell}} \frac{dr}{a_0} \left(\frac{r}{a_0}\right)^{3-2\pi K_0(T)} \tag{153}$$

These eqns are the analogues of the eqns (82) and (83) for $T(z)$ and $V_1(z)$ for the scattering problem. Now, we rescale things so that the integral in (152) goes back to the original limits; writing

$$\int_{e^{\delta\ell}}^{\infty} dx\, x^{3-2\pi K_0} \equiv e^{-(4-2\pi K_0)\delta\ell} \int_1^{\infty} du\, u^{3-2\pi K_0} \tag{154}$$

we can then rewrite (152) as

$$\tilde{K}^{-1}(T) = K_1(T) + 4\pi^3 y_1^2(T) \int_1^{\infty} du\, u^{3-2\pi K_0} \tag{155}$$

$$y_1(T) = e^{(2-\pi K_0)\delta\ell}\, y_0(T) \tag{156}$$

Let us now convert these results to differential eqns, using the infinitesimal nature of $\delta\ell$. We rewrite (153) and (156) as differential eqns, in exactly the same way we did for the scattering problem; the only difference here is that we now have 2 scaling variables $K^{-1}(\ell, T)$ and $y(\ell, T)$, and the differential

eqtn are now coupled. After trivial algebra, we get the famous KT scaling eqtns:

$$\frac{dK^{-1}(\ell,T)}{d\ell} = 4\pi^3 y^2(\ell,T)$$

$$\frac{dy(\ell,T)}{d\ell} = \left(2-\pi K(\ell,T)\right) y(\ell,T) \qquad (15Y)$$

Before we analyze these eqtns., it is useful to recall exactly what has been done here from a more physical point of view. We can see this by looking again at our fine-grained and coarse-grained pictures

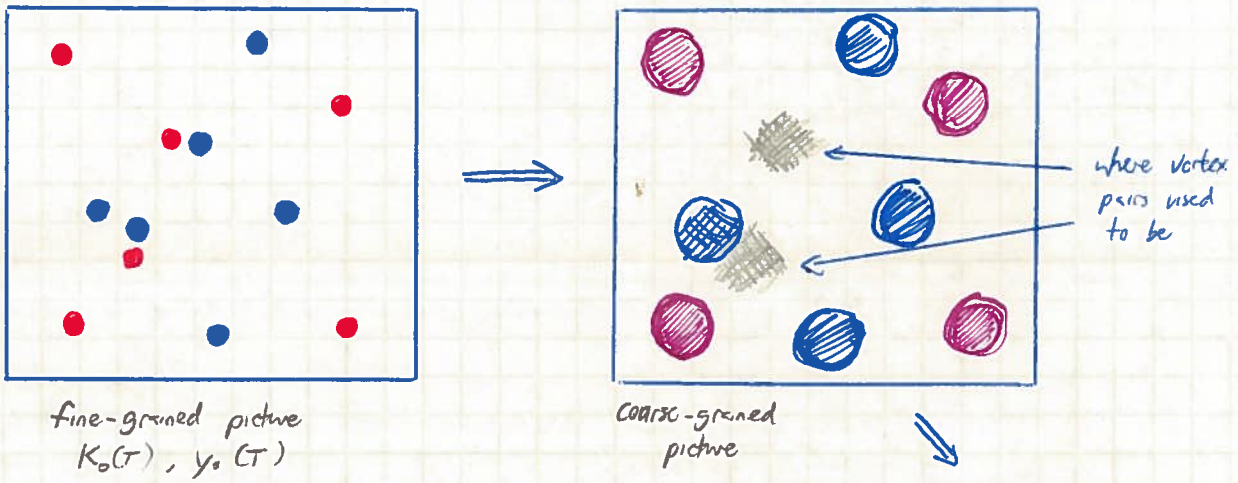

fine-grained picture $K_0(T)$, $y_0(T)$

coarse-grained picture

rescaled coarse-grained picture

$K_1(T)$, $y_1(T)$

The sequence of images shows how by first rescaling the lower lengthscale cut-off (ie., decreasing the resolution of our image) we remove close vortex pairs. Then by rescaling to attain the same apparent resolution, we get a new picture, with fewer vortices. We see it as though we had simply moved further away from the system!

This is not the only way that one may understand physically what we are doing here - another way is to look at the way the force between vortices renormalizes as we change the length scale. But we have perhaps said enough already - let us now proceed to the analysis of the scaling eqtns.

To analyze the scaling eqtns in (15Y), the easiest thing to do is to follow the flow as we change ℓ; we can almost do this by hand. Note that we clearly need to fix 2 boundary conditions, viz., an initial y_0 and an initial K_0. The eqtn for $y(\ell)$ shows that y either blows up exponentially or collapses exponentially, depending on whether the exponent $(2-\pi K(\ell))$ is greater than

or less than zero; and the first eqtn shows that if $y(\ell)$ blows up as $\ell \to \infty$, then $K(\ell)$ collapses. Thus we have a separatrix between the 2 behaviours, and further examination leads very quickly to the standard KT scaling graph:

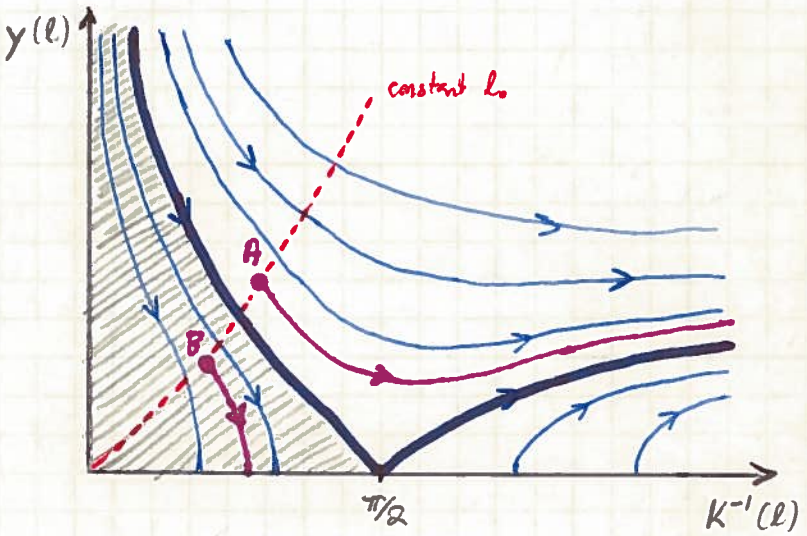

At left we plot the flow lines of the KT scaling eqtns; the separatrix between trajectories where $K^{-1}(\ell) \xrightarrow[\ell\to\infty]{} \infty$ and where instead $K^{-1}(\ell) \xrightarrow[\ell\to\infty]{} 0$ is shown in bold.

We also show specific trajectories with given initial starting points at A and B. The red hatched line refers to all trajectories with a given initial $\ell = \ell_0$

We see that the KT scaling diagram contains a lot of information. In the region to the left of the separatrix, $K^{-1}(\ell)$ scales to a finite value as $\ell \to \infty$. This finite value corresponds to a finite $\rho_s(T)$, and hence tells us that the system is superfluid, at least according to the criterion we defined above (viz., that $\chi_s(q,0) \neq 0$ in the $q \to 0$ limit). On the other hand trajectories to the right side of the separatrix scale so that $K^{-1}(\ell)$ goes to infinity with ℓ, so that $\rho_s \to 0$; the system is no longer superfluid.

It is illuminating to replot the KT scaling figure, both for y as a function of K and for μ as a function of K; these plot are shown below:

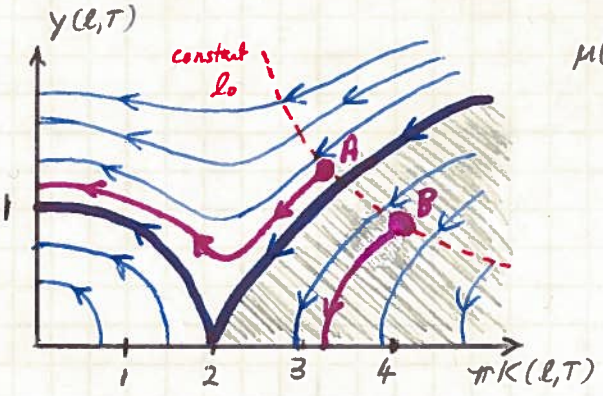

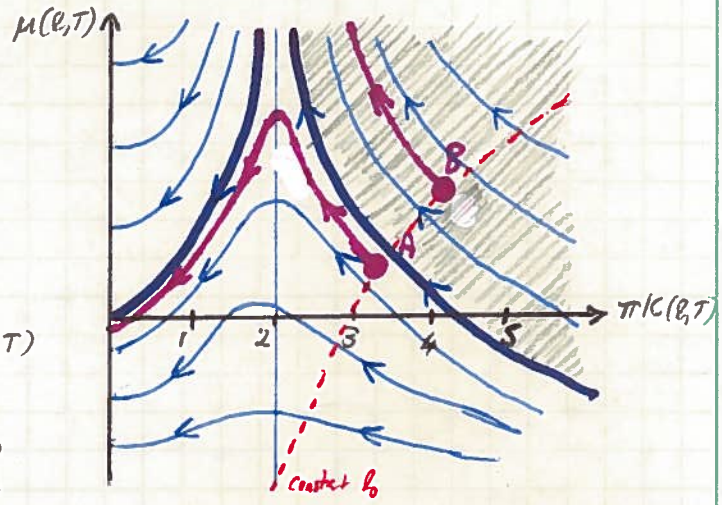

In all 3 cases we look at the scaling trajectories of 2 systems. One, system A, starts in the normal fluid regime - this is the high-T phase. The other, system B, starts in the low-T superfluid phase where they start depends things on kT, and on the initial lengthscale ℓ_0.

We can also ask what happens if we <u>stop</u> the scaling at a certain